

Chapter 1

Introduction

1.1 Preamble and Basic Definitions

The properties of impurities and defects are treated globally in textbooks dealing with the physical properties of semiconductors (for instance, [1] or [2]). An overview on the optical measurements on point defects in semiconductors is given in the chapter by Davies [3], and the relations between their optical properties and their colours in books dealing with colour in general, like the one by Nassau [4]. More ancient textbooks were devoted to the optical properties of semiconductors, for instance, the book by Moss [5], or aimed toward special topics like the vibrational absorption of impurities and defects in some insulators and semiconductors [6]. Many book chapters and reviews in journals have also been devoted to specific aspects of the absorption of impurities and defects and they are duly referenced in this book.

In this monograph, we consider first the electronic absorption of some kind of impurities and defects giving deep levels in the band gap of semiconductors and of covalent or partially covalent insulators. The electronic absorption of hydrogen-like centres in these materials was presented in a first book subtitled “I. Hydrogen-like Centres” [7]. The second point considered in the present book is the vibrational absorption of impurities and defects, electrically active or not, in the same materials.

Semiconductors differ from metallic conductors by the existence, at low temperature, of a fully occupied electronic band (the valence band or *VB*) separated by an energy gap or band gap (E_g) from a higher energy band empty of electrons (the conduction band or *CB*). When E_g reduces to zero, like in mercury telluride, the materials are called semimetals. In metals, the highest occupied band is only partially filled with electrons so that the electrons in this band can be accelerated by an electric field, whatever small it is. From a chemical viewpoint, most of these semiconducting and insulating crystals are elements or compounds in which all the valence electrons are used to form covalent or partially covalent chemical bonds, leaving no extra electron for electrical conduction. This is the case for the diamond form of carbon, for silicon and germanium, for many crystals resulting from the

combination of group IIB or IIIA elements of the periodic table with group V or VI elements (the II–VI or III–V compounds) or for the partially ionic IB–VII (e.g. CuCl) compounds. In purely ionic insulators, like sodium chloride, electron capture from the electropositive element by the electronegative one produces ions with closed shells. Values of band gaps of different semiconductors and insulators are listed in Appendix C.

From the optical side, the difference between semiconductors and insulators lies in the value of E_g . The admitted boundary is usually set to 3 eV (see Appendix A for the energy units) and materials with E_g below this value are categorized as semiconductors, but crystals considered as semiconductors like the wurtzite forms of silicon carbide and gallium nitride have band gaps larger than 3 eV, so that this value is somewhat arbitrary. The translation into the electrical resistivity domain depends on the value of E_g , but also on the effective mass of the electrons and holes and on their mobilities, and the solution is not unique; moreover, the boundary is not clearly set. “Semi-insulating” silicon carbide 4H polytype samples with reported RT resistivities of the order of $10^{10} \Omega \text{ cm}$ could constitute the electrical limit between semiconductors and insulators, but the definition of such a limit is finally of moderate importance. In the following, for simplification, “semiconductors and insulators” is generally replaced by “semiconductors”.

In a category of materials known as Mott insulators, like MnO, CoO, or NiO, with band gaps of 4.8, 3.4, and 1.8 eV, respectively ([8], and references therein), the upper energy band made from 3d atomic states of the metal is partially occupied and metallic conduction should occur. The insulating behaviour of these compounds is ascribed to a strong intra-atomic Coulomb interaction, which results in the formation of a gap between the filled and empty 3d states [9].

In pure covalent or partially covalent semiconductor crystals, a free electron is created in the CB once sufficient energy has been provided to a VB electron to overcome the energy gap E_g . The required energy can be produced thermally under equilibrium at temperature T , by optical absorption of photons with energies $h\nu \geq E_g$, or by irradiation with electrons in the keV energy range. These processes leave in the VB a positively charged free “hole”, noted h, which has no equivalent in metals, and whose absolute electric charge is the elementary charge. When free carriers can only be produced by the above processes, the semiconductors are said to be intrinsic. The electron–hole pair concentration n_i produced thermally in a semiconductor depends on the effective densities of states (DoS) N_c and N_v in the conduction and valence bands, which are temperature dependent, and on the band gap E_g . It can be expressed as:

$$n_i = (N_c N_v)^{1/2} \exp(-E_g / 2k_B T). \quad (1.1)$$

In germanium, silicon, and GaAs, at room temperature (RT), n_i is 2×10^{13} , $\sim 10^{10}$, and $2 \times 10^6 \text{ cm}^{-3}$, respectively. A consequence of the existence of an electronic band gap is that at sufficiently low temperature, the absorption of photon with energies below E_g by electronic processes does not occur in intrinsic semiconductors or insulators. Inversely, the photons with energies above E_g are strongly absorbed by

optical transitions between the valence and conduction bands, to produce electron–hole pairs, and this absorption is called fundamental or intrinsic.

Compound semiconductor crystals show strong infrared absorption in some spectral regions at photon energies below E_g due to the vibrations of the atoms of the crystal lattice. In these regions, the lattice absorption can be so strong that the crystals are opaque at usual thicknesses. At energies below the lattice absorption region, the crystals become transparent again. In elemental crystals like diamond (C_{diam}) or silicon, this first-order vibration of the lattice atoms is not infrared-active (there is no dipole moment associated to the symmetric vibration of two identical atoms) so that pure crystals of this kind do not become opaque, but they do show weaker absorption bands due to combinations of vibration modes of the crystal lattice.

Extrinsic semiconductors are materials containing foreign atoms (FAs) or atomic impurity centres that can release electrons in the *CB* or trap an electron from the *VB* with energies smaller than E_g (from neutrality conservation, trapping an electron from the *VB* is equivalent to the release of a positive hole in this otherwise full band). These centres can be inadvertently present in the material or introduced deliberately by doping, and the term extrinsic refers to the electrical conductivity of such materials. The electron-releasing entities are called donors and the electron-accepting ones acceptors. When the majority of the impurities or dopants in a material is of the donor (acceptor) type, the material is termed n-type (p-type) and the electrical conduction comes from electrons (holes). In doped semiconductors with $E_g \gtrsim 0.6$ eV, the intrinsic free-carrier concentration n_i can usually be neglected at RT compared to the extrinsic one. In these semiconductors, when the energy required to release a free carrier from the dominant donor or acceptor (the ionization energy) is comparable to the RT thermal energy (~ 26 meV), a measurement of the RT resistivity $\rho = (ne\mu)^{-1}$, where μ is the electrical mobility of the free carrier considered, gives a representative value of the concentration n of the dominant donor or acceptor.

For a semiconductor, the intrinsic resistivity $\rho_i(T)$ at a given temperature is determined by the concentration n_i of electron–hole pairs given by expression (1.1). For germanium, ρ_i is $\sim 50 \Omega \text{ cm}$ at RT, but it rises to $\sim 3 \times 10^5 \Omega \text{ cm}$ for silicon and to $\sim 10^8 \Omega \text{ cm}$ for GaAs. Above a temperature depending on the value of E_g , the concentration of electrons–holes pairs produced thermally by direct excitation through the band gap in extrinsic materials can become comparable to the extrinsic carrier concentration and the semiconductor is said to go into the intrinsic regime. The presence of free electrons produces at RT a Drude-type continuous optical absorption increasing as λ^2 , where λ is the wavelength of the radiation. The wavelength dependence of the free-hole absorption is not as simple. It must be pointed out that several residual impurities present in semiconductors are not electrically active and cannot be detected by electrical methods, so that the term intrinsic cannot be systematically taken as a synonym for high purity.

For some values of the donor or acceptor concentrations depending on E_g , the free-carrier absorption can be so large that the material becomes opaque in the whole spectral range. For still higher dopant concentrations, a transition to a quasi-metallic state (the metal–insulator transition) occurs.

When temperature is reduced, the free carriers in extrinsic materials are normally re-trapped by the ionized donors or acceptors centres, increasing the resistivity of the materials. The free carriers can also be trapped irreversibly by deep centres like transition metal (TM) atoms, native defects, or irradiation defects. This trapping can produce materials with RT resistivity close to the intrinsic one, and the spectroscopic properties of some of these deep centres are presented in Chap. 4.

A large number of semiconducting and insulating crystals are known which are used in various technologies and for pure and applied research, and most of them are grown artificially. All these crystals are made from or contain an element with more than one isotope. For specific applications, some of these crystals, like germanium, have been grown with a substantial enrichment in only one isotope, which can reach nearly 100%, and they are referred to in this book as quasimonoisotopic (qmi) crystals. Insulating crystals, either native or artificial are also used in jewellery, where their optical properties are of utmost importance.

1.2 Origins of Impurities and Defects

1.2.1 Natural Occurrence

Some insulating and semiconducting crystals, like diamond, various forms of silicon dioxide or corundum (Al_2O_3) are found in the native state. In some cases, the crystals are transparent (their band gap lies in the UV), but they can also come with different hues. One of the origins of these colours is the presence of FAs in the crystal lattice. These atoms originate from the presence of the corresponding chemical elements in the earth mantle during the formation of the crystals. One example is diamond, where the presence of a significant nitrogen concentration is responsible for the yellow hues of many natural diamonds. The type of natural diamonds and, by extension, of artificial ones is first determined formally by their overall nitrogen content as type I diamonds containing typically more than 1 ppm ($\sim 1.8 \times 10^{17} \text{ cm}^{-3}$) of N atoms and type II diamonds for the other crystals. This labelling is further refined by additional lettering bringing supplementary information. Thus, the rarely found natural type Ib diamonds contain only nitrogen atoms replacing carbon atoms (substitutional nitrogen), with an absorption onset toward higher energies at 2.2 eV ($\sim 564 \text{ nm}$), in the blue region of the spectrum, so that the complementary yellow colour, the canary yellow of the gemmologists, is preferentially perceived. The more common yellow type Ia diamonds contain, besides the so-called *A* aggregate (a pair of substitutional N atoms) and *B* aggregate [a missing atom (vacancy *V*) surrounded by four substitutional N atoms] the so-called N3 centre (VN_3) and the $(VN_2)^0$ centre. These latter centres have absorption lines in the visible (see Sect. 4.2) and their presence is responsible for the yellow colouration known as Cape yellow of these diamonds (Fig. 1.1).

All these N-containing diamonds are insulators, with resistivities in the $10^{15} \Omega \text{ cm}$ range, because the electronic levels introduced by nitrogen are

Fig. 1.1 The Allnatt diamond, weighing 101.29 ct (20.26 g), was cut from a stone assumed to come from South Africa. It is presently owned by the SIBA Corporation. This diamond is of the Ia type (G. Bosshart, private communication)



near midgap. N-lean diamonds are known as type II diamonds, and the purest ones are the colourless type IIa diamonds. The presence of boron in diamond produces a blue coloration due to the substitutional B acceptor and these natural type IIb diamonds are semiconducting, with resistivities as low as $5 \Omega \text{ cm}$ for a few natural stones. A discussion of the electronic absorption of type IIb semiconducting diamonds can be found in [7].

Blue-grey insulating diamonds have also been extracted from the Argyle mine in Australia and this colour has been attributed to high concentrations of hydrogen and of N-containing defects, together with the presence of Ni-related centres [10]. The colour of many natural diamonds is also affected by the plastic deformation they underwent during their growth and rise to the earth surface.

In a way similar to diamond, pure corundum (Al_2O_3) is colourless, but the presence of Cr^{3+} ions replacing Al^{3+} (typically a few percent) turn it into the red ruby while the presence of Fe^{2+} and Ti^{4+} ions gives the blue sapphire. Stable lattice defects producing colouration of the crystals can also be introduced in otherwise transparent minerals, like alkali halides, alkaline-earth¹ halides, or zircon (ZrSiO_4), and in diamond, by natural radioactivity. When crystals, like zircon, contain radioactive isotopes, the defects inducing colour are evenly distributed in the crystal, but when colour is due to external radioactivity, it is generally located in an outer region of the crystal corresponding to the penetration depth of the particles. In diamond, natural and artificial irradiations by neutrons, electrons, or γ -rays produce more or less intense green colouration of the stones due to the presence of vacancies and vacancy-related defects, and such irradiations are taken for responsible of the colour of natural diamonds like the so-called Dresden Green diamond shown in Fig. 4.12 [11]. These colour changes can arise from the selective absorption of light by impurities or defects in the crystal at the corresponding energies or from the

¹The alkaline earths are the atoms of column IIA of the periodic table (Be, Mg, Ca, Sr).

absence in the energy spectrum reflected by the crystal of a spectral domain which is absorbed by the crystal (see for instance, [4]).

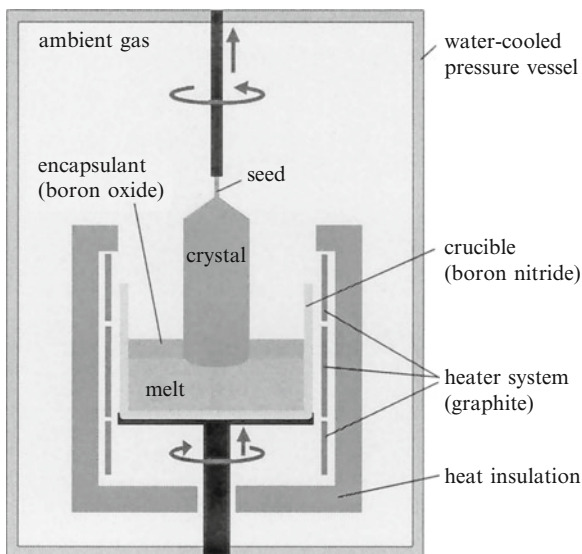
1.2.2 Contamination

The contamination by impurities of artificially grown materials can have several origins and some of them have been reviewed in [7] in relation to hydrogen-like (or effective-mass) centres. For bulk crystals, the impurities can come from their presence in the polycrystalline starting material used, as for carbon in silicon [12], from the growth atmosphere and/or, when a crucible is used, from chemical elements of the crucible containing the molten material. For instance, most of the silicon crystals used in the electronic industry are grown from a melt contained in a silica crucible by dipping a monocrystalline silicon seed just below the melt and slowly pulling it while silicon solidifies as a crystal at the seed bottom. This growth method, known as the Czochralski (CZ) method, after the Polish metallurgist Jan Czochralski [13], introduces in the silicon crystal a rather large concentration ($\sim 10^{18} \text{ cm}^{-3}$ or 20 ppma) of electrically inactive interstitial oxygen (O_i), originating from the partial dissolution or etching of silica by molten silicon ([14, and references therein]). The purest crucible-grown crystals are probably the undoped Ge crystals grown from a silica crucible in a hydrogen atmosphere by the CZ method, for which the overall bulk impurity concentrations (mainly Si, O and H) are in the 10^{14} cm^{-3} range [~ 2 atomic parts per billion (ppba)]. In the case of germanium, the much lower O contamination is due to its melting temperature (937°C) compared to 1414°C for silicon, and to the smaller affinity of O for germanium. Severe O contamination ($\sim 0.02\%$) also occurs in the high-pressure growth of GaN from a gallium solution containing dissolved nitrogen, probably due to the etching by ammonia of O-containing components of the apparatus. An indirect source of contamination arises when crystals containing an element with a high vapour pressure, like P or As, are grown by the CZ method: to prevent the evaporation of the volatile element, a compound with a low vapour pressure and a low miscibility with the melt of the crystal to be grown, the encapsulant, is placed at the top of the polycrystalline charge to be melted. Once molten, this encapsulant makes a tight seal between the molten material and the atmosphere of the furnace (usually nitrogen). This growth method is known as the liquid encapsulation Czochralski (LEC) method and Fig. 1.2 shows a schematic of a LEC crystal grower.

The price to pay is the unavoidable introduction in the crystals grown by this method of a small amount of atoms of the molten encapsulant: to grow GaAs and InP crystals, the encapsulant used is wetted boron oxide (B_2O_3). In addition to the introduction of B and O impurities, at high temperature, the water added to B_2O_3 to prevent sticking between the encapsulant and the crystal dissociates and hydrogen is introduced in the crystal [15].

A large concentration of hydrogen is also introduced in III–V layers grown by dissociation of organometallic compounds in the vapour phase epitaxial process ([16], and references therein).

Fig. 1.2 Schematic view of a liquid encapsulated Czochralski (LEC) crystal pulling machine showing the principle of the method. It is used to grow compound crystals like GaAs, where one of the constituents of the melt has a high vapour pressure. The rotation directions of the crystal holder and of the pyrolytic BN crucible are opposite. In the Czochralski technique used to grow CZ silicon, there is no encapsulant and the crucible material is silica



The contamination introduced by melting polycrystalline charges in a crucible at high temperature has led to the development of crucibleless growth methods for some crystals like silicon, when needed with a low O content for particular applications. In these methods, a monocrystalline seed is mounted at the bottom or at the top of a polycrystalline charge and the polycrystalline region in contact with the seed is melted by a contactless technique (RF field or halogen lamp furnace). The melted region is prevented to flow from capillarity forces alone and it is displaced upward or downward by moving the RF coil, leaving a monocrystalline region. This method, known as float-zone (FZ) growth method, was invented independently by several scientists ([17], and references therein). A schematic FZ setup for silicon crystal growth is shown in Fig. 1.1 of [14].

The growth of crystals with lower melting points and low reactivity has been obtained by the Bridgman method, named after the American physicist Percy Williams Bridgman, in an elongated crucible held horizontally, with the monocrystalline seed at one end of the crucible [horizontal Bridgman (HB) method]. The principle of the monocrystalline growth is to displace the molten zone from the seed region throughout the crucible length. The Bridgman method is also used in a variant where a sealed crucible is displaced vertically in a temperature gradient (vertical gradient freeze method), as for the growth of CdTe monocrystals [18]. With these methods, contamination of the crystals often occurs from the ambient gas.

Besides the nitrogen contamination due to the pollution of the carrier gas, the diamond films obtained by chemical vapour deposition (CVD) are usually contaminated with silicon. This can originate from the plasma etching of the silica walls of the reactor and from the commonly used silicon substrates [19].

Metallic contamination by TMs and Cu occurs in many semiconductors because of the high diffusion coefficients of these elements. This contamination can have

many origins including the initial purity of the materials, chemical etching, electrical contacts, mechanical contacts with metallic parts or metallic constituents of heating resistances in thermal treatments. For technological reasons, this contamination has been widely studied in silicon CZ wafers, and also in germanium, in relation to nuclear detectors. It remains usually at a low level, but it can be detected by very sensitive methods like deep-levels transient spectroscopy (DLTS), an electrical method, or, when the TMs complex with shallow dopants, by photo-thermal ionization spectroscopy (PTIS), which is related to optical spectroscopy. In the metal-solvent method of growth of synthetic diamond, graphite is first dissolved into a molten metal solvent like nickel, cobalt, or iron under high pressure and high temperature (HPHT) above the eutectic melting point of the solvent–carbon diagram, in a (P , T) region of the phase diagram of carbon where diamond is the stable phase (5.5 GPa and 1400°C are typical values). As more and more graphite is dissolved, the molten metal becomes supersaturated and small diamond crystals start to nucleate and begin to grow. Substitutional Ni and Co have been shown to be incorporated in diamond by this so-called HPHT growth method when nickel or cobalt is one of the solvent metals [20].

1.2.3 Doping

Doping consists in introducing into the crystal FAs called dopants which usually lower the resistivity of the intrinsic material and convert it into a well-characterized n-type or p-type material. However, doping of compounds semiconductors with TMs introducing deep levels in the band gap has also been used for optical purposes. The introduction of dopant atoms in III–V compounds is discussed in [21] and some aspects of doping are also discussed in [7]. Standard doping of bulk semiconductor crystals is achieved by adding either to the solid charge or directly to the melt a selected amount of the dopant element or of a crystal/dopant alloy. This method works for many dopants in group IV and in III–V semiconductors. However, the introduction of a FA in a crystal at a given concentration is determined primarily by its solubility. Moreover, it is not possible to dope any crystal with any impurity.

The possibility to use the transmutation of atoms of the crystals by thermal neutrons to dope semiconductors was first demonstrated by Cleland et al. [22]. A brief review of the possibilities of this method (neutron transmutation doping or NTD) and of its limits is given in [7]. A consequence of this doping method is also the introduction in the crystals of lattice defects produced by fast neutrons present in the neutron beam. These defects must be removed by annealing before using the semiconductor for the production of devices, and more is said below of these defects.

Doping can also be achieved by implantation in the crystals of dopant ions at energies typically below 100 keV, followed by thermal or optical annealing in order to remove lattice defects and produce dopant diffusion in the crystal. During the growth of epilayer by vapour-phase epitaxy, doping is also possible by adding to the gaseous flux organic molecules containing the dopant atom.

In some cases, the spectroscopic study of specific dopants and FAs with several isotopes has been facilitated by doping with a specific isotope or with an isotopic mixture enriched with one isotope.

1.2.4 Growth, Thermal Treatments and Irradiation

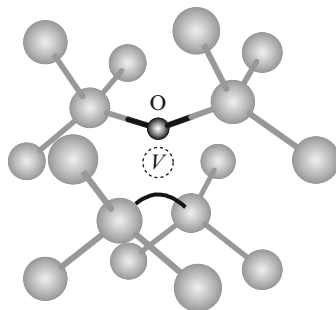
1.2.4.1 Growth and Thermal Treatments

The growth of crystalline samples or their annealing at very high temperature produces a steady-state concentration of elementary defects. The simplest ones result from the thermal ejection of a crystal atom from its crystal sites into an interstitial location. These self-interstitial atoms (I) leave an empty crystal site or vacancy (V). A slow cooling-down allows for recombination of the interstitial atoms into the empty sites, but a relatively fast cooling-down or a quenching allows the most stable of these defects to survive and/or to agglomerate at RT. This is the mechanism put forward to explain the origin of point defects produced during the growth of some III–V and II–VI compound crystals under stoichiometric conditions, where anion and cation vacancies, as V_{Cd} or V_{Te} in CdTe, can be produced, as the cooling-down of the solidified fraction is not an equilibrium process. In CZ silicon crystals, depending on the pulling rate and on the thermal gradient at the solid/liquid interface, excess vacancies or interstitials are present. They are mobile and some V – I pairs can recombine, but in regions presenting a vacancy excess, the vacancies agglomerate to form macroscopic voids which can be present in CZ, and also FZ silicon crystals at concentrations $\sim 10^4$ – 10^7 cm^{-3} [23, 24]. CZ void-free silicon crystals can be grown by adjusting the pulling rate and the temperature gradient at the solid/melt interface ([25], and references therein). In regions with excess of interstitials, extended defects can be produced, like series of dislocation loops, best known as striations or swirls, which are decorated by oxygen in CZ silicon. In GaAs crystals grown by the HB or LEC methods, and also in epitaxial layers grown by CVD, several native defects are present, including the EL2 centre [26, 27].

The main native defects in III–V and II–VI compounds are vacancies and atoms in antisites. For instance, the As antisite (As_{Ga}) as well as the As vacancy (V_{As}) are residual defects in LEC-grown GaAs crystals [27]. ZnO is a material whose electrical properties are determined by native lattice defects: the presence of interstitial Zn correlated with that of O vacancies (V_{O}) seems to be responsible for the n-type electrical conductivity of many crystals, but in high-resistivity crystals obtained by hydrothermal growth, the dominant defect is V_{Zn} [28].

Last, but not least, annealing of CZ silicon or O-containing germanium in the 350–500°C temperature range produces several O-related electrically active centres known as thermal donors (TDs), and their atomic structures differ as a function of the annealing duration. One category, which involves only O and Si or Ge atoms in the cores of the centres are thermal double donors (TDDs) that can bind two extra electrons [29, 30]. In CZ silicon containing N or H, short-time annealing in the 300–600°C range produces also donors known as shallow thermal donors

Fig. 1.3 Atomic structure of the VO centre in silicon. The O atom is bonded to two nearest neighbours of the vacancy and a bond is reconstructed between the two other nearest neighbours. There are six equivalent orientations for this centre about the central vacancy



(STDs) [31]. The electronic spectra of these donor centres are discussed in Chap. 6 of [7] and their vibrational spectra in Chap. 6 of the present volume.

1.2.4.2 Radiation Defects

The radiation defects in semiconductors started to be investigated in the 1950s to elucidate their effects on semiconductor devices exposed to high-energy (h-e) particles, including specifically semiconductor detectors for h-e particles, and later in processes like NTD. Defects can be deliberately introduced in semiconductor and insulator crystals by irradiation with h-e photons (γ rays or X-rays), elementary particles, or ions. Irradiation with γ rays, h-e electrons and fast neutrons, protons or α particles (He nuclei) has been adopted for the deliberate production and study of lattice defects in covalent and partially covalent materials. Combinations of irradiations and thermal treatments are also used to colour gemstones by introducing lattice defects or complexes with absorption lines or bands in the visible region of the spectrum.

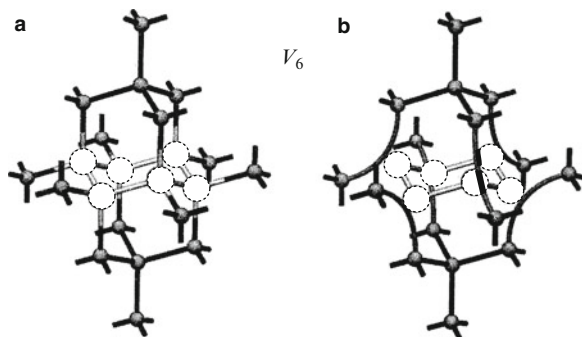
The penetration depth of the particles depends on their charge, on their energy, on their mass, and on the atomic number of the crystal target. The charged particles interact mainly with the electron cloud of the atoms or ions of the crystal and for the same energy, their penetration depth is much smaller than that of neutrons, which interact mainly with nuclei.

For irradiation with h-e nucleons, the primary defects produced depend on the energy, charge, and mass of the particles. In covalent crystals, the simplest primary defects produced by γ -ray or electron irradiation are I and V .

In silicon, vacancies produced by electron irradiation near 10 K start diffusing near 150–180 K in p-type and near 70–80 K in n-type material. During their diffusion, they can interact with impurities and defects. For instance, in silicon, two vacancies can combine to form a divacancy² usually noted V_2 ; vacancies can also get trapped by dopant atoms to give V -dopant pairs, or with an interstitial O atom (see [33]) to form the oxygen-vacancy centre (VO), represented in Fig. 1.3, which is stable up to $\sim 300^\circ\text{C}$.

²The divacancy is also produced as a primary defect in neutron-irradiated silicon [32].

Fig. 1.4 Schematic diagram of the hexavacancy (V_6) in silicon. The missing atoms are the *large light balls* showing the location of the vacancy sites in a puckered hexagonal configuration. (a) Unrelaxed. (b) With six reconstructed bonds. V_6 displays a trigonal symmetry about the vertical $\langle 111 \rangle$ direction [38]



VO , also known in silicon as the A centre, can be also considered as a limiting case of substitutional oxygen when the O atom comes close to the vacancy site [34]. The vibrational properties of this centre in silicon and germanium are discussed in Sect. 7.1.

Besides V_2 , which is stable up to $\sim 200^\circ\text{C}$, irradiation of silicon with fast neutrons can also produce polyvacancies, and indirect evidence for the formation of trivacancy (V_3) has recently been given [35]. Calculations have predicted that the hexavacancy (V_6) is a very stable defect in silicon [36, 37] and it is shown in Fig. 1.4.

An unattributed photoluminescence (PL) line observed a long time ago in heat-treated neutron-irradiated silicon has been ascribed to V_6 [38]. Vacancies have been mainly studied in diamond and silicon after their production by electron irradiation, but there is a difference between the two crystals: in diamond, V is stable up to $\sim 600^\circ\text{C}$ while in silicon it is only stable below RT. Many other complexes involving lattice defects are known in semiconductors and insulators.

Protons are hydrogen nuclei so that irradiation with h-e protons introduces not only lattice defects but also hydrogen in the irradiated crystal. This hydrogen can “decorate” lattice defects produced by the implantation by forming H bonds whose vibrations can be detected by optical spectroscopy. The fully hydrogenated vacancy VH_4 where the four dangling bonds of a vacancy are saturated by a H atom is such an example [39]. A combination of proton implantation and thermal annealing of CZ or FZ silicon has also been shown to produce shallow donors [40]. Hydrogen can also be introduced in a region near from the semiconductor surface by hydrogen plasma treatments as long as the semiconductor surface does not suffer excessive plasma etching.

1.3 Structural Properties

1.3.1 Global Atomic Configurations

In crystals, FAs can take simple configurations, but depending on their concentration, diffusion coefficient, or chemical properties and also on the presence of different kind of impurities or of lattice defects, more complex situations can be found. Aside from indirect information like electrical measurements or X-ray diffraction, methods such as optical spectroscopy under uniaxial stress or a magnetic field, electron spin resonance, channelling, positron annihilation, or extended X-rays absorption fine structure (EXAFS) can bring more detailed results on the location and atomic structure of impurities and defects in crystals. We describe here the simplest atomic configurations. In the course of the chapters, more complicated configurations will also be met and discussed.

In the simplest case, a FA can replace an atom of the crystal at a regular lattice site. It becomes then a substitutional impurity or dopant, noted with index s in the general case (e.g. B_s). In covalent or partially covalent crystals, the main relevant parameters for the possible location of a FA on a substitutional site are its ability to form chemical bonds with its nearest neighbours (nns), the strengths of these bonds, and the difference between the atomic radius of the FA and that (or those) of the crystal atoms. When a crystal is made up of two different elements, like one with the sphalerite or wurtzite structure, a substitutional FA can in principle occupy two different lattice sites. Sometimes, depending on its concentration and on the growth conditions, the same atom can occupy in fact two different lattice sites. This kind of amphoteric behaviour occurs, for instance, in GaAs, a cubic crystal with sphalerite structure, where, depending on the growth conditions, a Si atom can occupy either a cation site (Si_{Ga}) where it is a donor or an anion site (Si_{As}) where it is an acceptor.³ This duality is not a general rule, however, and, for instance, the doping or contamination of GaAs with C produces only C_{As} . In heteropolar semiconductors, each kind of atoms of the crystal occupies one sublattice (the group III and the group V sublattices in III–V compounds). For different reasons, it can occur that some group V (III) atoms get located on group III (V) sublattice and these already-mentioned antisite atoms can be considered as “internal” impurity atoms. Similarly, a foreign group III atom can occupy a group V site (B in GaAs, for instance) and act as an “external” antisite. The location of FAs at substitutional sites is very common among semiconductors and insulators. This does not necessarily mean that the FA takes the exact equilibrium position of the atom it replaces as, depending on the radius and valence of the FA, lattice distortion can occur that will be discussed later. Besides well-defined crystal structures like sphalerite and wurtzite where there is only one substitutional site for each kind of atom, there

³With reference to chemistry, when considering a binary compound, the site of the metal atom is called the cation site and the other one the anion site.

are more complicated structures like the polytypes found, for instance, in the SiC compound, where there can be several kinds of substitutional sites differing by the symmetry of their *nns* (see Appendix B).

Small FAs tend to occupy interstitial sites, but some of them can also locate in the same material on a substitutional site, as lithium in GaAs. Figure 1.5 shows possible interstitial locations of isolated FAs in a III–V compound with sphalerite structure.

In the T_i sites, the impurity is located at a tetrahedral interstitial site, where it is weakly bonded to the crystal lattice. In compounds with the sphalerite or wurtzite structure, in which there are two different substitutional sites, there are also two different T_i sites: one where the interstitial atom is nearer from atoms of one sublattice and another where it is nearer from atoms of the other sublattice ($T_{i\text{ III}}$ and $T_{i\text{ V}}$ of Fig. 1.5). As the electronic densities at these two sites are different, the interstitial atoms occupy preferably one of these sites. This T_i location is also met for Li atoms in silicon and germanium, and as there is no chemical bond between the Li and Si or Ge atoms, the $2s$ valence electron of Li has a low binding energy, making interstitial Li (Li_i) a shallow donor in these semiconductors. In the interstitial bond-centred (BC) location, bonding must be rearranged to allow the FA to form chemical bonds with its neighbours. Besides a rather small size of the

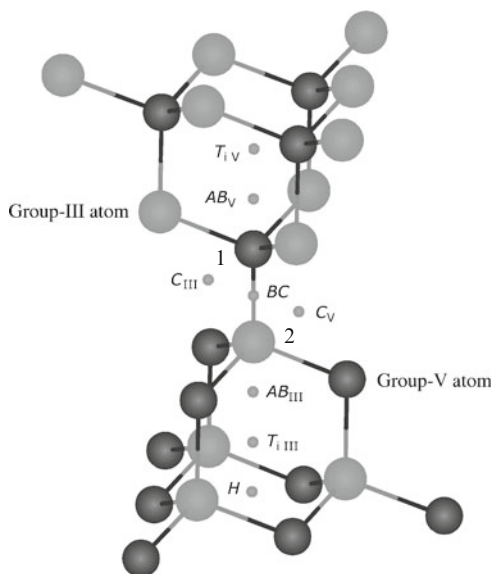


Fig. 1.5 High-symmetry interstitial sites (*small spheres*) in a III–V sphalerite lattice oriented along a $\langle 111 \rangle$ vertical axis (the simple substitutional sites of the crystal atoms are not indicated). The bond-centred (BC), antibonding (AB), tetrahedral interstitial (T_i) and hexagonal (H) sites are located along the $\langle 111 \rangle$ axis. The T_i and AB sites are noted according to the atoms closest to these sites. The C site, midway between two next nearest neighbours along a $\langle 110 \rangle$ axis, is noted according to these atoms. The M site (not shown) is midway between two adjacent C_{III} and C_{V} sites and also midway between a BC site and a H site

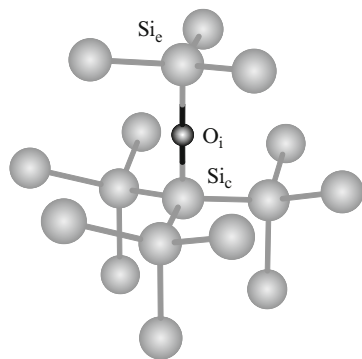
atom, this latter location also implies a strong affinity between the foreign and lattice atoms. The paradigm of such a structure is isolated interstitial oxygen (O_i) in silicon (Fig. 1.6). Low-temperature vibrational absorption spectroscopy shows that in the static configuration, the Si–O–Si geometry is puckered, with an apex angle of $\sim 162^\circ$ (see Fig. 6.1) but the mixed rotation-tunnelling motion of O_i in a plane perpendicular to the $Si_c \cdots Si_c$ axis leads to a dynamical configuration where the probability of presence of O_i is maximum on the $Si_c \cdots Si_c$ axis, as shown in Fig. 1.6.

The above example introduces a more general property of impurities and impurity complexes in crystals, namely, orientational degeneracy. In the linear configuration of Fig. 1.6, the four equivalent $\langle 111 \rangle$ orientations of the Si–O–Si structure around the central Si_c atom are equally populated and display the same vibrational properties: this structure displays therefore a fourfold orientational degeneracy. For centres with noncubic symmetry in cubic crystals, orientational degeneracy is the rule and it can be extrapolated to other crystal structures. A value of the energy required to jump from one orientation to an equivalent one (the reorientation energy) can be of interest to determine some physical properties of the centre, such as the diffusion coefficient, and it is shown later in the book how it can be measured.

An interstitial atom in an antibonding (AB) site is bonded to its nearest neighbour lattice atom. This location is often found for H in complexes involving a donor atom and it results in the relaxation of the local lattice bonding. Special interstitial structures like the di-interstitial configuration are discussed later in this book. Incidentally, Fig. 1.5 emphasizes the ternary symmetry of the sphalerite lattice along a $\langle 111 \rangle$ direction. It allows to see the analogy with the wurtzite structure, where the $\langle 111 \rangle$ direction is replaced by the c -axis direction (Appendix B). In the $\langle 111 \rangle$ direction, the sphalerite lattice is made of alternate layers of atoms of the two sublattices. It can also be seen in Fig. 1.5 that the stacking sequence is a period of three layers of the same kind (the so-called ABC sequence).

Pairing between identical or different FAs is also found in semiconductors and insulators, depending on factors, which can be inter-related, and several pairing configurations can be met. We limit ourselves here to the description of the simplest

Fig. 1.6 Dynamical location of isolated interstitial oxygen in a silicon crystal (see text). The two Si atoms bonded to O are represented in the same plane as their neighbours because of the repulsion induced by the O atom. There are four equivalent orientations of O_i in the crystal around the central Si_c atom



ones, and others will be eventually considered later. In elemental semiconductors, the simplest kind of pairing concerns impurities on *nn* substitutional sites or *nn* substitutional and interstitial sites, and the atoms of the pair are generally different. Another important kind of pairing found in silicon concerns two identical or different FAs located on equivalent distorted interstitial sites. This is illustrated by the location of nitrogen in N-containing silicon and germanium because of the relatively small size of the N atom compared to the lattice atoms, and also because of the high strength of the N_2 molecular bond. In these crystals, most of nitrogen goes in the form of a nitrogen split pair depicted schematically in Fig. 1.7. In this configuration, with C_{2h} symmetry, the two N atoms are located at equivalent distorted interstitial sites and they are bonded to their three *nn* Si atoms. They are separated from each other by two quasi-substitutional Si atoms (atoms 4 and 5 in Fig. 1.7), to which they are bonded. This trivalent bonding is the natural one of N in many molecules, and it makes this N_i-N_i pair, known as a split pair, electrically inactive.

Complexes similar to this N_i-N_i pair, where one of the N atoms is replaced by a C or an O atom, have been identified in silicon and they will be discussed in due time. A second atomic geometry has also been investigated by Jones et al. [41] for the nitrogen split di-interstitial, based on a model proposed as a building block of the platelets in diamonds assuming that they were made of nitrogen, called the Humble model [42]. This latter configuration, with C_{2v} symmetry and consisting of two [011] *nnn* split interstitials, is shown in Fig. 1.8. For N_i-N_i in silicon, the energy of this structure was found to be 0.9 eV larger than the one of Fig. 1.7, but it is found to be the most stable configuration for the diamagnetic self-di-interstitial in diamond [43].

In compound semiconductors, the same kind of pairing as in elemental semiconductors can be found, with the addition of pairs of identical or different *nnn*

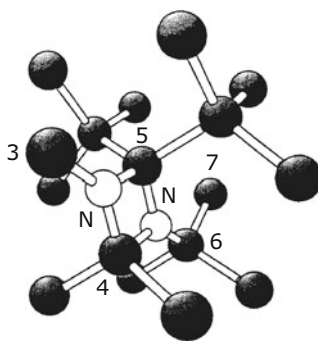


Fig. 1.7 Model of the nitrogen split pair (N_i-N_i) in the silicon crystal. In the perfect crystal, the Si atoms 3, 4, 5, 6, and 7 form a zigzag chain along a $\{110\}$ direction in a $\{110\}$ plane. The introduction of the two N atom leads to the breaking of the Si-Si bonds between atoms (3, 4), (4, 5), and (5, 6), and to the bonding of one N to atoms 3, 4, and 5 and of the other N to atoms 4, 5, and 6 (after [41])

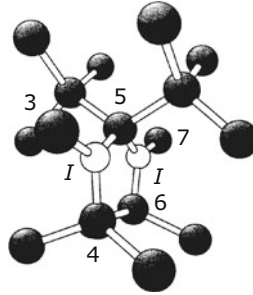


Fig. 1.8 Humble model of a split di-interstitial structure in the diamond lattice. The introduction of two interstitial atoms I (in white) leads to the breaking of the bonds between atoms (3, 4), (4, 5), (5, 6), and (6, 7), and to the rebonding between atoms 4 and 6. In this model, the two I atoms are bonded to five lattice atoms (after [41])

atoms on the same sublattice. For instance, in GaP, N is an isoelectronic FA with a relatively high solubility and at concentrations larger than $\sim 10^{17} \text{ cm}^{-3}$, it can first form the so-called NN_1 pair due to nnn N_P atoms and when increasing $[\text{N}]$ to more distant NN pairs, whose spectroscopic properties were investigated by Thomas and Hopfield [44].

Pairing can be due to the interaction between atoms of opposite type, like for the donor–acceptor substitutional mn pairs found at high dopant concentrations in silicon [45] or nnn B_P –chalcogen pairs in GaP [46]. Another kind of pairing is a mixed one between a substitutional acceptor atom (actually a negative ion) and a positively charged interstitial atom. The $\text{Li}_\text{i}^+ \text{B}_\text{s}^-$ pair is an example of such a configuration, but many other pairs involving interstitial TM ions also exist. The mobility of interstitial atoms produced by electron irradiation can also result in pairing: in electron-irradiated silicon containing carbon, evidence of the presence of a mixed $\text{C}_\text{i} \text{C}_\text{s}$ pair has been obtained, related to the difference of electronic charge of the two atoms. A limiting case of pairing is that of the interstitial hydrogen molecule found in different semiconductors after hydrogen-plasma treatment, which is a nearly free rotator ([47], and references therein).

1.3.2 Lattice Distortion and Metastability

FAs in a crystal can induce a local distortion of the lattice. When they are substitutional, this is caused by the difference between their atomic radii and those of the atoms they replace, and also by their chemical affinity with the surrounding atoms. According to Vegard’s law,⁴ substitutional atoms having a smaller (larger) atomic

⁴Vegard’s law is an empirical rule which holds that an approximate linear relation exists between the crystal lattice parameter of an alloy and the concentration of its constituent elements ([48]. See also [49]).

radius than the atom they replace should produce a uniform lattice contraction (expansion) of the crystal proportional to their concentration. With reference to the unperturbed lattice parameter a_0 of cubic crystal, the change Δa of the lattice parameter produced by a concentration N_f of FAs can be expressed as:

$$\frac{\Delta a}{a_0} = \beta_f N_f, \quad (1.2)$$

where β_f is the lattice contraction or expansion coefficient. For substitutional impurities in covalent or partially covalent cubic crystals, the sign and an order of magnitude of β_f can be obtained by replacing Δa by the difference between the covalent radii of the impurity and of the atom of the host crystal it replaces, a by the intrinsic atomic separation in the host crystal and N_f by the number of available sites for impurity sites per unit volume [50]. The value of this coefficient for substitutional C in silicon, calculated from the atomic radii, is $\beta_{C(\text{calc})} = -6.85 \times 10^{-24} \text{ cm}^3 \text{ atom}^{-1}$. For dopants with a covalent radius showing a large difference with that of the atom it replaces, like Tl or Bi in silicon, or P in diamond, this distortion puts a limitation to their solubility. Another kind of local distortion met for substitutional impurities is a lowering of symmetry like the one for isolated N in silicon or diamond, where this atom is displaced along a N–X bond (X is an atom of the crystal) along a $\langle 111 \rangle$ direction. A local distortion can also reduce the symmetry of a centre through the Jahn–Teller effect, as for the atomic vacancy in silicon: this defect should normally display tetrahedral symmetry, but it is lowered to D_{2d} , and this can be detected in the paramagnetic states by the dependence of the ESR spectra on the magnetic field orientation (see for instance [3] of appendix B, p. 467, of this reference). Lattice distortion related to the bond lengths can also occur for an interstitial atom strongly bonded to atoms of the crystal in the BC configuration of Fig. 1.6. In this particular case, if the structure remains linear, the two nn atoms of the crystal can be pushed out from their equilibrium positions when the lengths of the new bonds exceed the equilibrium nn separation.

When the local effect of distortion and the impurity concentration are large, a difference in the average lattice parameter as a function of the impurity concentration can be measured with appropriate X-ray diffraction techniques. In silicon, values of $\beta_C = -6.9 \times 10^{-24} \text{ cm}^3 \text{ atom}^{-1}$ and $\beta_O = 4.4 \times 10^{-24} \text{ cm}^3 \text{ atom}^{-1}$ have been measured for C_s and O_i , respectively [51, 52]. One can note incidentally the good agreement between the measured value of β_C and the value predicted from Vegard's law. With $[O_i] \sim 10^{18} \text{ cm}^{-3}$ found in most CZ silicon crystals, the value of β_O corresponds to a relative increase of the lattice parameter of 4.4×10^{-6} compared to high-purity FZ silicon.

The lattice distortions induced by substitutional impurities can also be measured locally from the distance between an impurity atom and its nearest neighbours using EXAFS [53]. The results of the EXAFS experiments require sensible interpretations as they do not necessarily follow simple rules like the addition of the covalent radii of the elements involved [54, 55]. Local volume changes of group V and group VI

donor atoms in silicon have been obtained indirectly from a comparison between the measured spacings of the electronic absorption lines of these donors with calculated values [56]. Interesting conclusions concerning the change of colour of ruby as a function of the chromium concentrations have been also drawn from EXAFS measurements [57]. Global lattice expansion or contraction can be also measured, for instance, by X-ray diffraction, in doped layers epitaxied on an undoped substrate of the same material from the positive or negative interface stresses, depending on the atomic radius of the doping atom with respect to that of the atom it replaces. In some cases, first-principle calculations have given a good insight of the local distortion induced by a foreign atom [58, 59].

For centres with different charge states (they will be fully discussed in the next section), the distortion can be modified by a change of the electronic density in the vicinity of the centre. The consequence is that a change of the charge state of a centre can produce a local lattice relaxation. It is usual to describe the electronic energy states of these centres as a function of configuration coordinates. When a change of the charge state induces lattice relaxation, the equilibrium configuration coordinates differ in the two states (see Fig. 1.9). It should be noted that, within the same global charge state of a centre, due to differences in electronic densities, lattice relaxation can also occur between the ground state and excited states, with the same consequences regarding the equilibrium configuration coordinates.

A limiting case of distortion is the occurrence of a second atomic configuration of a centre in the same charge state. The idea of this possibility was not obvious at first sight, but experimental results including optical spectroscopy results have led to admit this situation. When two such non-degenerate atomic configurations of a centre coexist, the one with the lowest energy is the stable one and the second is said to be metastable. There is an energy barrier between the two configurations and its value determines the temperature domain of the metastability. The corresponding centre is often said to be bistable. An example of such a bistable centre is the B_s-Si_i (BI) pair, produced in B-doped silicon by electron irradiation at low temperature, which is discussed in Sect. 7.1 in relation with its vibrational absorption.

The change of configuration of a centre induced by its transition into a metastable state produces a lattice distortion which can result in a macroscopic volume change. Transient effects due to the photocreation of electron-hole pairs in n-type GaP and SI GaAs have been attributed to this effect [60].

1.4 Physico-chemical Properties

1.4.1 Solubilities

In many cases, impurities and dopants are introduced in the molten phase, in which they have a definite solubility $N_{\text{sol-1}}$. In the solid phase, near from the melting

point, the solubility $N_{\text{sol-s}}$ decreases with respect to the liquid phase and the ratio $N_{\text{sol-s}}/N_{\text{sol-l}}$ is the segregation (or distribution) coefficient, which is usually less than unity. The solubility of impurities in crystals can be considered, in most cases, as the maximum concentration of isolated FAs which can be introduced in the crystal before precipitation, formation of cluster of a mixed compound (e.g. SiC in C-doped silicon) or of an alloy. The solubility of an impurity is conditioned by characteristics such as its atomic radius, electronic structure, site(s) in the crystal, eventual binding energies with the atoms of the crystal, and tendencies to complex or to form pairs. As it generally requires energy to introduce an impurity in a crystal, solubility is a temperature-dependent (thermally activated) process characterized by an activation energy (the heat of solid solution), and for this reason, it is larger near the melting point of the crystal than at RT. When a solubility is mentioned, it is therefore mandatory to know to what temperature it corresponds. For solubilities measured near RT, one must distinguish between the equilibrium solubility, which correspond to a cooling down of the crystals after the introduction of the FAs under conditions close to thermodynamic equilibrium and non-equilibrium solubility. In the second case, the apparent solubility is larger than the equilibrium solubility and the crystal is oversaturated. This situation is met naturally for O_i in CZ silicon. There has been many studies of the solubility of O_i in silicon (see [61] for a review) and the equilibrium solubility $[\text{O}_i]_s$ between the melting point (1414°C) and 850°C can be reasonably represented by [62]:

$$[\text{O}_i]_s \text{ (cm}^{-3}\text{)} = 9.0 \times 10^{22} \exp[-1.52 \text{ (eV)} / k_B T]. \quad (1.3)$$

Within these limits, the solubility calculated using expression (1.3) varies between 2.6×10^{18} and $1.4 \times 10^{16} \text{ cm}^{-3}$. There is no exact value of the equilibrium solubility of O_i at RT, but it is expected to be lower than the value at 850°C. $[\text{O}_i]$ measured at RT in CZ silicon is none the less in the 10^{18} cm^{-3} range, showing an oversaturation of this material with O_i . Comparable values have been reported in O-doped germanium [63]. In silicon, nitrogen is not a residual impurity because its solubility is much smaller than that of the other group-V elements and of carbon and oxygen. One of the reasons for this can be the fact that its most stable configuration in silicon is the N pair presented above. As nitrogen doping improves the mechanical properties of silicon, its doping has been actively investigated. Non-equilibrium solubilities of dopants can also be deliberately reached after implantation by solid-phase-epitaxial regrowth, flash or laser anneals of the implanted zone. These fast annealing procedures produce a local out-of-equilibrium situation which is frozen at RT because of the very short cooling-down duration. The metastable solubilities obtained by such annealings can be one order of magnitude larger than the equilibrium solubilities [64]. The problem of the solubility of FAs in a crystal can be complicated by the fact that the same atom can sometimes occupy either interstitial or substitutional sites, like some TMs in silicon. In that case, the apparent solubility is larger for the interstitial location. Globally, the TMs are characterized by a solubility in the 10^{16} – 10^{17} cm^{-3} range and by diffusion coefficients significantly larger

than those of the substitutional shallow donors and acceptors (see [65] for a review). The interstitial solubility of TMs and of group-IB elements in silicon, also depends on the concentration of substitutional acceptors in the material because, as mentioned before, they can form interstitial–substitutional pairs with these acceptors. This is also true from Li_i , which form pairs with substitutional acceptors, but there seems to be no consensus on the RT solubility of Li_i in FZ silicon. A value $\sim 10^{16} \text{ cm}^{-3}$ can be inferred from the conclusions of [66]. As a rule, the solubility of elements of groups II and VI in silicon decreases compared to that of elements of group III and V, with the notable exception of O and H. The solubility of C in III–V compounds has been thoroughly investigated because in these crystals, C is in some cases a pollutant and usually a p-type substitutional dopant with a rather large solubility limit (in the 10^{20} cm^{-3} range for GaAs). In silicon the solubility of substitutional C at the melting point is $\sim 4 \times 10^{17} \text{ cm}^{-3}$ [67] and it is larger in CZ silicon than in FZ silicon because the lattice contraction induced by C_s is compensated by the lattice dilatation induced by O_i . In crystals supersaturated with C, annealing can produce the precipitation of SiC microcrystals [68].

Besides the substitutional/interstitial location of the same FA, other centres can exist where more than one FA are involved, like the *nn* substitutional pairs for chalcogens in silicon or nitrogen in diamond so that in these cases, one must consider a global solubility of the FAs.

In most crystals supersaturated with substitutional or *BC* impurities, these atoms are usually immobile at RT because their diffusion coefficients are small at this temperature. However, when annealing is performed at relatively high temperatures where materials are still saturated with impurities, precipitation or formation of complexes involving impurities can take place because of their migration. This is the case in CZ silicon, where silica precipitates are produced during annealing at 800°C. Attempts to introduce high C concentration in silicon crystals, lead also to the already-mentioned precipitation of SiC microcrystals.

It is clear that a solubility limit can no longer be defined when the host crystal and the impurity are partially or fully miscible. This is the case with Ge in silicon, giving at high Ge concentrations $\text{Ge}_x\text{Si}_{1-x}$ alloys, and also with most of the group III FAs in III–V compounds, like Al in GaAs giving $\text{Al}_x\text{Ga}_{1-x}$ As alloys.

1.4.2 Diffusion Coefficients

At the atomic scale, the diffusion of a FA in a crystal lattice can take place by different mechanisms, and the most common in silicon and germanium are the vacancy and interstitial mechanisms. The interstitial/substitutional or kick-out mechanism, which is an interstitial mechanism combined with the ejection of a lattice atom (self-interstitial) and its replacement by the dopant atom is also met for some atoms like Pt in silicon.

When the constant surface concentration of an impurity with diffusion coefficient D is N_{is} , its concentration $N_i(x, t)$ at depth x from the surface of a plane sample of thickness $d \gg x$ after a diffusion time t is given in the ideal case by:

$$N_{ix} = N_{is} \operatorname{erfc} \frac{x}{2\sqrt{Dt}}, \quad (1.4)$$

where the complementary error function $\operatorname{erfc} u = (1 - \operatorname{erf} u) = 2/\sqrt{\pi} \int_x^\infty e^{-t^2} dt$. The error function $\operatorname{erf} u$ is tabulated p. 142 of the book by Runyan [69].

The temperature dependence of the diffusion coefficient is generally expressed as:

$$D(T) = D_0 \exp[-E_D/k_B T], \quad (1.5)$$

where E_D is an activation energy related to the diffusion mechanism. In Table 1.1 are listed values of D_0 and E_D for a few representative dopants and impurities in silicon. Values of D for many other FAs in silicon can be found in [78].

At a given temperature, in a cubic crystal, an order of magnitude of the atomic jump rate of a diffusing atom between two atomic sites (the number of jumps per unit time) is D/a_0^2 , where a_0 is the lattice constant of the crystal. From the above value of D for the P atom in silicon at 1200°C, this jump rate is $\sim 400 \text{ s}^{-1}$ for the P atom. For interstitial atoms like Li_i or BC interstitial O, see Part IV of [79]. The value of the diffusion coefficients of impurities and dopants in semiconductors can be modified by the presence of compensating impurities or of crystal dislocations so that the interpretation of diffusion measurements requires some thought. This is also the case for the diffusion of hydrogen in silicon, whose values depend on the doping type and doping level, because of the possibility of pairing with the dopant atoms [80]. Finally, it must be mentioned that as the diffusing species can be ions, the diffusion coefficient can be modified by an electric field.

Table 1.1 Values of diffusion parameters of some representative foreign atoms in silicon

FA	References	D_0 (cm^2s^{-1})	E_D (eV)	D (cm^2s^{-1})
Al	[70]	1.8	3.2	2×10^{-11} (1200°C)
P	[71]	5.3	3.69	1.2×10^{-12} (1200°C)
S	[72]	0.047	1.8	3.3×10^{-8} (1200°C)
Li_i	[73]	2.5×10^{-3}	0.655	4.4×10^{-9} (300°C)
Cu_i	[74]	4.5×10^{-3}	0.39	1.7×10^{-6} (300°C)
Fe_i	[75]	9.5×10^{-4}	0.65	1.5×10^{-6} (900°C)
Ti_i	[76]	0.0145	1.79	1.1×10^{-8} (1200°C)
Pt	[65]	5.9	3.97	1.5×10^{-13} (1200°C)
O_i	[62]	0.13	2.53	2.9×10^{-10} (1200°C)
C	[77]	1.9	3.1	4.7×10^{-11} (1200°C)

D is calculated at the temperature indicated in parentheses using expression (1.5)

1.5 Electrical Activity

1.5.1 Donors and Acceptors

In a semiconductor or an insulator, a centre can be considered as electrically active if it can display more than one electronic charge state. This is the case when electrons or holes are either released from the centres with energies smaller than the band gap or trapped by the centres. This can occur for many FAs, but the substitutional FAs with one more (or less) valence electron than the atom they replace are of particular importance as their bonding with their *nns* leaves an extra electron not involved in the bonding or is completed by the borrowing of a valence electron of the crystal, leaving a positive hole. The FAs belonging to the first kind are called donors (D) and those belonging to the second kind, acceptors (A). The Coulomb interaction between the positive (negative) foreign ion and the extra electron (hole) has led to compare these centres with hydrogen-like (H-like) atoms. The main difference between these H-like atoms in semiconductors and in atomic physics comes in the former case from their embedding in a crystal matrix with static dielectric constant ϵ_s , from the mass of the electron, different from the mass m_e of free electron in vacuum, or from the “mass” of the positive hole. In a first step of the modelling of the properties of H-like centres, the relevant masses are replaced by scalar “effective” masses m_e^* or m_h^* , for electrons and holes, respectively. This is an oversimplification, but scalar values of the effective masses can be obtained from a modelling of the RT electrical measurements. The factor scaling the energy of these centres with the Lyman energy spectrum $E_{0n} = R_\infty/n^2$ of H in vacuum is $s = (m^*/m_e)/\epsilon_s^2$, where m^* is the appropriate effective mass. The energy E_n of the effective-mass centre is thus $1.36 \times 10^4 s/n^2$ (meV), where n is the usual principal quantum number. This is the basis of the effective mass theory (EMT), which is presented in detail in Chap. 5 of [7]. Within this approximation, the ground state energy or level for the acceptors in silicon ($m_h^* \cong 0.6m_e$, $\epsilon_s = 11.7$) is separated from the *VB* continuum by 60 meV, and for the donors in GaAs ($m_e^* \cong 0.07m_e$, $\epsilon_s = 12.9$) by 5.7 meV from the *CB* continuum. These values are orders of magnitude of the ionization energies of the shallowest of these centres, known as shallow centres, but the crude assumptions made cannot account for the effect of the chemical nature of the impurity on the ionization energies, which can be important for semiconductors like silicon. The technological importance of the shallow donors or acceptors is that they bind electrons or holes with energies comparable to the RT thermal energy (~ 26 meV). Thus, the carriers released at RT by these shallow centres act as a reservoir to control the electrical conductivity of the crystals. Under equilibrium, this release is a thermal process and as the electrons and holes are particles with non-integer spins, their energy distributions follow Fermi–Dirac statistics. At a given temperature T , the concentration of electrons and holes in the continua can be expressed as a function of the chemical potential μ of the semiconductor. In metal physics, the Fermi level E_F is the energy of the electron level whose occupancy probability is 1/2 and it has the same meaning as the more

general chemical potential. The term “Fermi level” has been extrapolated from metal to semiconductor physics, despite the fact that in semiconductors, E_F lies in the band gap, where there is only a limited number of discrete allowed states. Here, to comply with the common use, we keep “Fermi level” which is at best a quasi-Fermi level.

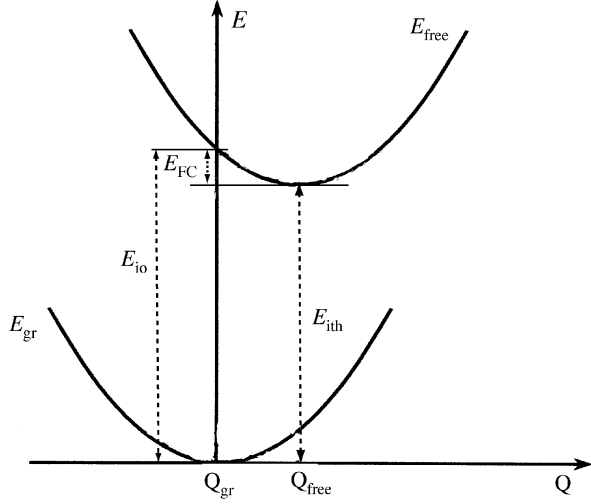
At very low temperature, the concentration of free carriers in the continuum is negligible as they are trapped by the ionized impurities of the opposite charge and E_F is close to the energy level E_i of the dominant impurity. This level separates the band gap into two regions: one, between E_i and the relevant band continuum, taken as the energy origin and a second one for energies between E_i and the opposite band continuum. In energy diagrams for single donors (D) or acceptors (A), the zone contiguous to the opposite continuum is noted “+” for donors and “−” for acceptors as, when E_F lies in this zone, the centre is ionized (D^+ or A^-). In the same spirit, the second zone is noted “0” because when E_F lies in this zone, the centre is neutral (D^0 or A^0).

There are also FAs with two more (or less) valence electrons than the lattice atom they replace, which act as double donors (DD) or acceptors. In group IV semiconductors, this is, for instance, the case for the chalcogen atoms (S, Se, and Te) belonging to group VI of the periodic table, with three charge states DD^0 , DD^+ and DD^{++} . $(DD)^0$ can be first ionized to give DD^+ , with an ionization energy substantially higher than the one for single donors, and DD^+ can in turn be ionized with an energy approximately two times higher than the one for DD^0 . In this aspect, they can be considered as some kind of He-like centres.

The H-like and He-like centres do not show much lattice relaxation between the neutral ground state and ionized states and the ionization energies measured electrically or spectroscopically are about the same. For deep centres, where a substantial lattice relaxation can occur between the ground and ionized states, the energies can be represented approximately in 1D by parabolas as a function of a general lattice (configuration) coordinate representing the lattice relaxation between the two states (Fig. 1.9). The threshold of the optical transitions (optical ionization energy E_{io}) takes place without lattice relaxation while the thermal ionization energy E_{ith} corresponds to an equilibrium configuration and Fig. 1.9 shows that in this particular situation, E_{ith} is smaller than E_{io} . The difference is the Franck–Condon shift. Such a diagram is called a Huang–Rhys diagram and it will be used later with some additions in the discussion of the coupling of the electronic transitions of impurities with phonon modes of the crystal.

These deep centres can still be considered as donors or acceptors, but in that case, a donor is better defined as a hole trap and an acceptor as an electron trap. The trapping and emission efficiencies of these centres are quantified by captures and emission cross-sections for electrons or holes. Some centres with capture cross-sections not too dissimilar for electrons and holes, as substitutional Ag or Au in silicon, are sometimes called amphoteric, by analogy with the chemical terminology. The term amphoteric has also been used to describe the same impurity in different lattice sites, where it can display either acceptor or donor properties (e.g. Si in GaAs). The separation between shallow and deep centres is an oversimplification as there are also centres in between.

Fig. 1.9 Configuration coordinate Huang–Rhys diagram of the electronic energies of an impurity centre whose lattice equilibrium configurations in the ground and ionized states are represented by configuration coordinates Q_{gr} and Q_{free} with different values. The thermal ionization energy E_{ith} of such a centre is smaller than the optical ionization energy E_{io} by the Franck–Condon energy E_{FC}



1.5.2 Compensation

In a real semiconductor, more than one kind of donor and acceptor impurities are usually present at the same time, but to simplify, we start considering a material containing only one kind of FAs of each type. The one with the highest concentration N_{maj} is the majority impurity, which determines the electrical type of the semiconductor and the other is the minority impurity with concentration N_{min} . The net concentration of active centres able to contribute each a free carrier is $N_{\text{maj}} - N_{\text{min}}$ and this comes from the annihilation of a concentration N_{min} of electron–hole pairs. This situation is called compensation, and it can also arise from the presence of centres in concentration N_{trap} which can trap carriers from the majority impurity. The compensation ratio K is usually defined as the ratio $N_{\text{min}}/N_{\text{maj}}$. When the intrinsic concentration of electrons and holes can be neglected, this net concentration is close to the free carrier concentration measured when these active centres are thermally ionized, or to the number of neutral centres which can be spectroscopically detected at low temperature under thermal equilibrium. Between the low-temperature region where the electron concentration n in a n-type semiconductor is practically zero and the exhaustion region where it is $N_{\text{maj}} - N_{\text{min}}$, the temperature dependence of the electron concentration n released in the CB by the donor with ionization energy E_i is:

$$n = \frac{N_{\text{maj}} - N_{\text{min}}}{N_{\text{min}}} N_c e^{E_i/k_B T}, \quad (1.6)$$

where N_c is the effective DoS in the CB. A similar equation holds for the hole concentration p in the VB in a p-type semiconductor, by replacing N_c by the effective DoS N_v in the VB. Expression (1.6) shows that for shallow impurities,

E_i can be derived from $n(T)$ and it can be obtained, for instance, from the temperature dependence of the Hall coefficient $R_H = -r/ne$ (the Hall factor $r = \langle \tau^2 \rangle / \langle \tau \rangle^2$ depends on the electron or hole scattering process through their lifetime τ , and in most semiconductors, it is close to $3\pi/8$). An alternative is a measurement of the energy absorption spectrum of the hydrogen-like impurities at low temperature, from which ionization energies can be extrapolated and this method is fully explained in [7].

Compensation reduces the concentration of active majority impurities, but it produces also additional impurity ions of both charges. These ions are the source of the so-called ionized impurity scattering for the majority free carriers and it reduces their lifetime. The electrical conductivity of a crystal is proportional to the number of free carriers and to their electrical mobility, which is in turn proportional to their lifetime. As a consequence, in the extrinsic regime, a high resistivity (or a low value of the carrier concentration measured directly from Hall effect) does not necessarily mean a high purity of the material.

We have mentioned the situation where a dopant atom can locate on two different sites where it behaves either like a donor or an acceptor. For some growth conditions, this possibility can produce what is known as self-compensation, and this occurs indeed for GaAs:Si. Another example of self-compensation is the doping of ZnO with Li: this results in a material with a relatively high resistivity, attributed to the occupancy with comparable probabilities by a Li atom of interstitial sites, where it acts as a donor, and of Zn sites, where it is an acceptor.

The actual compensation in a material is more complex than a simple balance between a majority impurity and a minority impurity as the material usually contains a combination of residual impurities, dopant and deep centres, whose concentrations must be estimated to know the actual degree of compensation in the material. As said before, compensation of majority impurities by adding opposite-type dopant or by the presence of deep centres leaves in the material charged ions, which reduce the lifetime of the free carriers. When the carrier lifetime in a given pure material is known, a lifetime measurement of an unknown sample of this material can inform on the degree of compensation of the sample.

1.5.3 Passivation

In the compensation process, there is only a change in the charge state of the impurity or dopant atom and it is temporarily reversible, for instance, by illumination of the crystal with band gap or above-band gap radiation. This illumination produces electrons and holes that are trapped by the ionized centres. This is of course an out-of-equilibrium situation, which prevails only during illumination.

When studying the interaction of hydrogen plasmas with crystalline silicon surfaces, it was discovered that hydrogen could penetrate in the bulk of the material and decrease its electrical conductivity [81, 82]. What could have been due to a compensation effect revealed itself as a passivation effect where hydrogen interacted

chemically with the shallow acceptors in silicon to form electrically-inactive centres. This was reminiscent of older studies which had showed that hydrogen played a role in the passivation of deep centres at the Si/SiO₂ interfaces and later on bulk and interface defects in crystalline silicon, not to mention the role of hydrogen in amorphous silicon. A proof of this interaction with shallow acceptors in silicon was the observation of IR vibrational modes related to hydrogen–acceptor complexes. These complexes were electrically inactive so that they did not contribute to the ionized impurity scattering. This process has naturally been called passivation and it has been observed for many donors and acceptors in semiconductors (see, for instance, [39], and references therein). However, the interaction of hydrogen with impurities in semiconductor crystals is complex and in some cases it can turn electrically inactive impurities into electrically active complexes. Moreover, for double donors or acceptors, it can passivate partially the centre and turn a deep impurity into a shallow donor or acceptor complex. These points are discussed in Chap. 8.

1.5.4 Deep Levels and Negative- U Properties

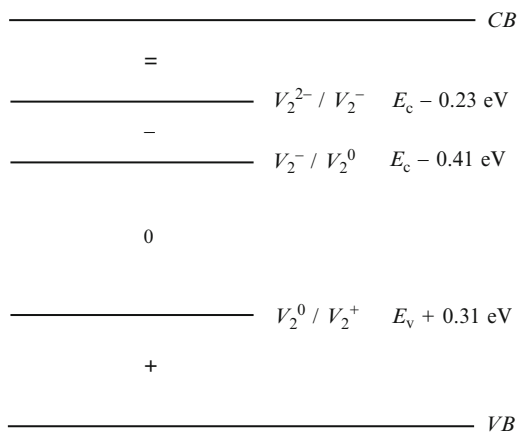
Many impurities and most defects complexes give electrical levels deep in the band gap, whose excited states cannot be considered as EM states. When ionization of these centres in the continuum takes place, the measured thermal ionization energy is smaller than the optical one because of the Franck–Condon shift. The thermal ionization energies of these deep centres are usually measured by transient capacitance methods like deep-level transient spectroscopy (DLTS) rather than from the temperature dependence of the Hall effect because the former technique is easier to use and more adapted to the problem when deep levels are involved.

In a semiconductor, a neutral double donor (acceptor) atom can release two electrons (holes) into the conduction (valence) band. The ionization energy of the first particle is smaller than that of the second one as the energy of the centre binding two particles is smaller than the one when it binds only one particle. This can be understood considering the Coulomb repulsive energy between the two electrons or the two holes. In defect physics, the energy difference between the second particle and the first one is sometimes called the Hubbard correlation energy (noted U) and in the above example, it is positive. For a centre like a double donor, the band gap of the semiconductor is thus separated into three energy regions by the DD^+/DD^0 and DD^{++}/DD^+ ionization energies of the donor. With the same meaning as that for single donors, the energy region from the CB (E_c) to the DD^+/DD^0 level is noted “0” and the two other ones similarly “+” and “++” in order of increasing energy. For a double acceptor, the sequence would be “0”, “–”, and “—” in order of increasing energy with respect to the VB (E_v). Such an ordering characterizes positive- U centres and most of the multicharged centres enter this category. For instance, the already-mentioned divacancy V_2 , produced in silicon by electron or neutron irradiation, is stable up to about 250°C, but in an initially p-type material, it

can trap a hole, giving V_2^+ . Inversely, in initially n-type material, it can trap one or two electrons to give V_2^- or V_2^{2-} . This defines three energy levels in the band gap: a V_2^{2-}/V_2^- “double acceptor” level, a V_2^-/V_2^0 acceptor level, and a V_2^0/V_2^+ “donor” level. The sequence of the charge states zones of V_2 in the silicon band gap is shown in Fig. 1.10. There is some spread in the values of the energy levels of V_2 in silicon and those given in Fig. 1.10 are those quoted by Svennson et al. [83]. More details on this defect are given in Chap. 4.

It turns out that for a few multicharged centres, the energy is larger with respect to the conduction (valence) band when the number of electrons (holes) bound to the centres is the largest. Following the suggestion of Anderson [84] applied to chalcogenide glasses, this can be explained by the gain in energy provided by a large lattice relaxation between the two charge states. With the above convention, the correlation energy U of these centres is negative and they are known as negative- U centres. Within the double donor model used above, the DD^0/DD^+ level should then be deeper in the band gap than the DD^+/DD^{++} level. In the case of negative- U properties, this ordering as function of energy is no longer possible and when two such DD^+ centres are present, their energy can be minimized by turning them into one DD^0 and one DD^{++} centres, which are the only stable charge states. It looks as if the two energy levels were replaced by a virtual DD^0/DD^{++} one, halfway between DD^0/DD^+ and DD^+/DD^{++} . An example of negative- U centre is off-centre oxygen (O_{oc}) in GaAs, also known as $V_{As}O$. This defect, produced when oxygen is present during the growth of GaAs crystals, contains an off-centre O atom bonded to two next- nn Ga atoms. It can be detected by the vibrational absorption of the Ga–O–Ga mode [85] and its absorption spectroscopy is presented in detail in Sect. 7.3. The two stable charge states of the centre are $V_{As}O^-$ and $V_{As}O^+$. As for other negative- U centres, the “forbidden” charge state, here $V_{As}O^0$, is metastable at low temperature and it can be produced by capture by $V_{As}O^+$ of electrons produced by photoionization of other defects. It has been thought for some time that the atomic configuration of this centre was the analogue in GaAs of the VO centre

Fig. 1.10 Charge states sequence of the divacancy V_2 in silicon showing the charge state of V_2 when the Fermi level is located in a given energy zone of the band gap. E_c and E_v are the respective positions of the conduction band (CB) and valence band (VB). The values of the V_2^{2-} and V_2^- energy levels are those quoted by Svennson et al. [83]



in silicon or germanium, with O and V_{As} as the only ingredients. However, on the basis of total energy calculations [86] and of the absence of atomic reorientation, the two other neighbours of V_{As} are likely to be As_{Ga} antisite atoms instead of Ga atoms. Another example of negative- U centre is the one known as interstitial B in silicon discussed in Sect. 1.3.2 in relation with metastability [87, 88].

1.5.5 Transition Metals

TMs are elements with an incomplete d or f electron shell. The $3d$ TMs go from Sc to Cu, the $4d$ ones from Y to Ag, and the $5d$ from Hf to Au [elements of column IB (Cu, Ag and Au) are included in the TMs despite full d shells because of the presence of only one ns electron]. As the electrical properties of the TMs are rather different from those of the impurity elements of columns II, III, IV, V and VI of the periodic table, we present here some facts that are indirectly related to their electrical properties, but can clarify them, despite the fact that they have already been mentioned in this chapter. Compared to usual dopants, TMs are connected to the neighbouring lattice atoms by a rather strong short-range potential and they can therefore give deep levels in the band gap. In group IV crystals, some of them can be found indifferently at substitutional and interstitial sites, with different electrical properties, while others, like Fe, are found only at interstitial site. For instance, the diffusion coefficient is generally much larger at interstitial than substitutional locations, but it must be kept in mind that the measured diffusion coefficients of the TMs depend on several parameters, an important one being the initial doping of the material. The high diffusion coefficients of some TM ions and their positive charge states result in the formation of pairs between the interstitial TMs and negative acceptor ions as well as with other substitutional impurities. This is a well-documented phenomenon, especially for Fe in silicon [89]. No general rules, however, exist concerning the diffusion coefficients of interstitial TMs in silicon as, although some elements like Fe and Cu show large diffusion coefficients, interstitial Ti, for instance, is a very slow diffuser (Table 1.1). In silicon, substitutional Au is amphoteric, with an acceptor level 0.61 eV above the VB and a deep donor level 0.79 eV below the CB . In III–V and II–VI crystals, the TMs replace the metal cation. The typical solubilities are in the 10^{16} – 10^{18} cm $^{-3}$ range, with some exceptions like Mn or Co, which have much larger solubilities or can even form definite compounds with group VI elements (the band gap of MnTe is ~ 1.3 eV). The III–V and II–VI alloys with Mn and Co belong to the category of diluted magnetic semiconductors. These materials offer perspectives in the domain of spintronics and their properties are actively investigated [90].

In a chemical description of the III–V and II–VI compounds, the metalloid atoms contribute five or six electrons to the crystal bonding and the metals three or two atoms, respectively. Consequently, the different charge states of the TMs are often described starting from an ionic description of the neutral TM atoms M omitting the electrons involved in the bonding. This is of course an approximation as the above

crystals are partially covalent. In III–V and II–VI compounds, the neutral states are therefore noted M^{3+} and M^{2+} , respectively.

The following concerns III–V compounds, but it can be extrapolated, *mutatis mutandis*, to II–VI materials. In the same way as a neutral acceptor atom in silicon can be ionized by trapping an electron, a M^{3+} ion in a III–V compound can trap an electron to give M^{2+} . The energy change from M^{3+} to M^{2+} corresponds to the M^{2+}/M^{3+} acceptor level (M^-/M^0 in the usual shallow impurities description), but in contrast to the shallow impurities description, the level is considered as empty in the M^{3+} state. The same applies for the M^{4+}/M^{3+} (M^+/M^0) donor level. Depending on the initial availability of free electrons or holes in the material, several charge states of the same TM element can be detected: for instance, introducing vanadium in p-type GaP results in the observation of a deep V^{4+}/V^{3+} donor level at $E_v + 0.2$ eV while doing the same in n-type material allows a deep V^{3+}/V^{2+} acceptor level at $E_c - 0.58$ eV to be observed.

The absolute energy levels of impurities are related to vacuum instead of the valence or conduction band of the host crystal. These absolute values require knowing the VB energy of the crystal with respect to vacuum. This latter energy is the work function or photothreshold of the crystal, i.e. the energy Φ to photoionize an electron from the VB into vacuum (in GaP, for instance, Φ is ~ 6.0 eV, compared to 7.5 eV in ZnS and 5.2 eV in silicon). The absolute energy levels of the impurities are thus obtained by subtracting from Φ the energy levels related to the VB . It has been found that for a given TM in compound materials, the absolute energy levels for different host crystal with the same formal composition (i.e. III–V compounds or II–VI compounds) are roughly the same. For instance, the absolute V^{3+}/V^{2+} levels in GaP and GaAs are 4.3 and 4.2 eV, respectively. In semiconductors with a wide band gap like GaP or ZnSe, it is possible to find both the TMs donor and acceptor levels in the band gap, but when the gaps are smaller, only one level lies generally in the band gap. The other level is resonant with the valence band or the conduction band. This is the case with the V^{3+}/V^{2+} acceptor level in InP, which is resonant with the CB . This alignment of the TMs energy levels with respect to vacuum is very useful to predict such resonances.

1.5.6 Attracting Isoelectronic Impurities

When a FA from the same column of the periodic table replaces an atom of the crystal, it is in principle electrically inactive because both atoms have the same number of valence electrons. Such a FA is referred to as an isoelectronic atom, and in most cases, it is indeed electrically inactive. In a III–V compound, the substitution of an atom of the group III sublattice by another group III atom does not modify the electrical properties of the compound (at least as long as the foreign group III atom can be considered as an impurity and not as a component of an alloy). We have mentioned the role of the atomic potential in the immediate vicinity of the impurity site. It can occur that, for some isoelectronic impurities or

for some electrically inactive complexes, the combination of the atomic potential with the potential produced by the local lattice distortion produces an overall electron- or hole-attractive potential. This potential can bind electrons or hole to the neutral centre with energies much larger than those for shallow electrically active acceptors or donors. In a semiconductor containing such isoelectronic centres, a free exciton (FE) (an electron-hole pair stabilized by Coulomb interaction) produced at low temperature by band gap illumination can therefore be trapped by these centres because of the preferential interaction with the electron (resp. hole) part of the exciton. The hole (electron) part of the exciton is then comparable to a hole (electron) bound to a negatively (positively) charged acceptor (donor) ion. This metastable entity is therefore called a pseudo-acceptor (resp. pseudo-donor). The study of excitons bound to isoelectronic centres in silicon and compound semiconductors (isoelectronic bound excitons or IBE) was actively investigated in the 1980s. In compound semiconductors, one of the best-studied electron-attractive (pseudo-acceptor) is probably N_P in GaP [44]. Isoelectronic substitutional oxygen can also play this role in some II–VI compounds ([91], and references therein). Bi at a P site in GaP and InP seems to be the best-documented hole attracting centres [92, 93]. In silicon, the potential near a C or Ge atom cannot bind an electron or a hole and electrically active isoelectronic centres are complexes like the Be pair at a Si site [94], or some (C, O) complexes in irradiated or annealed CZ silicon which are discussed in Sect. 6.1 of [7].

1.5.7 Lattice Point Defects

The simplest lattice point defect in covalent or mostly covalent crystals is the already-mentioned atomic vacancy V . In silicon it is stable only at low temperature and for a convenient study, it is produced by irradiation below typically 20 K, but in diamond (C_{diam}), it is stable up to ~ 870 K ($\sim 600^\circ\text{C}$). In n-type silicon, V can trap an electron to become V^- , which is paramagnetic, giving the Si-G2 ESR spectrum. V^- starts migrating at about 70 K. In p-type silicon, there is also an ESR evidence of V^+ . The correlation between the charge states of V in silicon and the electronic levels in the band gap is far from simple. The position of the two donor levels V^0/V^+ and V^+/V^{++} are close to the valence band, but the study is complicated by the negative- U character of V^+ . The positions of the V^-/V^0 and V^{2-}/V^- acceptor levels have not yet been established, except for the tentative conclusion that the V^{2-}/V^- level is deeper than 0.17 eV from the CB [95]. The electron or neutron irradiation of n- or p-type silicon near RT always lowers the electrical conductivity of the material. This indicates the production by irradiation of lattice defects and impurity-defect centres that act as traps for the donor electrons and acceptor holes. The creation of majority deep traps by h-e irradiation is not a general rule, however, and a counter-example is that of n-type germanium: under electron or neutron irradiation at RT, the electrical conductivity of this material starts first

decreasing, but under larger fluences,⁵ the conductivity goes p-type and it increases again with increasing fluences. This is attributed to the formation of a V_2 -donor complex with acceptor levels ~ 0.1 eV for V_2 -P, V_2 -As, and V_2 -Sb [96].

1.6 Optical Properties

The optical properties of impurities and defects are mainly studied by optical absorption, PL, or Raman scattering usually performed in reflexion geometry. Schematically, in the absorption measurements, the sample is inserted between a radiation source, which can be made monochromatic before or after the sample, and the transmission of the sample is measured as a function of the energy of the radiation by the appropriate radiation detector. In PL, the sample is illuminated by a relatively intense monochromatic radiation source and the radiation emitted by the sample analysed as a function of energy. In the Raman scattering measurements, the sample is excited at oblique incidence with a laser line at a given energy and the scattered radiation is usually analysed at 90° from the direction of the laser beam with the appropriate monochromator. In measurements performed at RT, the lines scattered at energies higher (anti-Stokes spectrum) and lower (Stokes spectrum) than that of the laser line can be detected, but in the Raman measurements performed at low temperature, only the Stokes spectrum is observed. In that latter case, the energies of the Raman transitions are the differences between the energy of the laser line and those of the Stokes spectrum.

The observed spectra can be continuous or discrete, but for identification or structural studies, the discrete spectra bring more information, especially when the lines are sharp. Precious information on the chemical nature and atomic structure of the centres is obtained from isotopic effects. For pure electronic transitions, called zero-phonon lines (ZPL), these isotopic effects are small.

1.6.1 Electronic Studies

Many impurity and defects centres are electrically active, displaying more than one charge state, and electronic absorption of one of these charge states is generally observed. Electronic absorption of the above-described H-like donor or acceptor centres when neutral is observed in the infrared at low temperature. It is characterized by a line spectrum converging with increasing energy into a continuous spectrum called the photoionization spectrum. Besides the ionization energies of the centres, the parameters for these spectra are those of the conduction and valence bands of the host crystal for the donors and the acceptors, respectively. For this

⁵The fluence of an irradiation is the total number of particles per unit area incident on the sample.

reason and in the absence of accidental resonances with the phonon spectrum of the host crystal, in a given material, the spectra of the different donor centres are very similar, the only difference being the energy region where the spectrum occurs, and this is also true for the spectra of the different acceptor centres. The spectroscopy of these centres, which can also include PL spectra, has been widely investigated and it is presented in details in [7].

The FEs can bind to neutral H-like centres with electron-hole binding energies E_{ex} slightly larger than that of the FEs. The difference is called the localization energy E_{loc} of the resulting bound exciton (BE). Excitons are created by laser illumination of a semiconductor sample at an energy larger than E_{g} and the study of their radiative recombination by PL has been an active field of the optical spectroscopy of semiconductors [97–99]. The excitons can recombine radiatively by emitting a photon at energy $E_{\text{gx}} = E_{\text{g}} - E_{\text{ex}}$. However, in indirect-gap semiconductors, conservation of the momentum of the weakly bound electron, comparable to that of a free electron, implies the creation of a lattice phonon of opposite momentum so that the energy of the photon emitted is $E_{\text{gx}} - E_{\text{phon}}$ where E_{phon} is the energy of the momentum-conserving phonon. In indirect-gap semiconductors, this phonon-assisted process has a significantly larger intensity than the zero-phonon intensity. Besides the phonon-assisted replicas, the recombination of excitons bound to complexes with internal vibration modes can take place with the excitation of some of these modes, producing what are known as vibronic sidebands.

In ionized deep centres, free electrons or holes produced by above-band gap excitation can be trapped in shallow excited states, from which they recombine radiatively to the ground state. This PL process is known as internal luminescence, and it provides a way to measure the ionization energy of the deep centre when the energy of the shallow state is known.

1.6.2 *Vibrations of Impurities and Defects*

The presence in a crystal lattice of FAs bonded to atoms of the crystal introduces perturbations in the lattice periodicity. These perturbations are due to local changes in the atom masses (in most cases), in the bond lengths and in the force constants between the atoms. When the mass differences and the difference with the crystal bonding are small, the main result is a perturbation of the one-phonon mode distribution of the perfect crystal, with additional features from the local disturbance. One then speaks of resonant modes, which can propagate at some distance of the FAs and give rise to IR absorption below the Raman frequency of the crystal (the maximum one-phonon frequency). The resonant modes have been mainly studied in elemental semiconductors as, contrary to compound materials, the former do not show one-phonon absorption and allow absorption measurements in the vicinity of the Raman frequency [100]. In some compound semiconductors where a phonon gap exists, some impurity vibrational modes can lie in this gap. They are then localized and are known as gap modes. When, for comparable or

smaller FAs masses, the bonds with the FAs are stronger than the crystal bonds, the frequencies of the induced modes are above the Raman frequency and they do not propagate in the crystal. Such modes are known as localized vibrational modes (LVMs) and most of them are IR-active. These LVMs are observed whatever the electrical activity of the centres and their study is the only possible spectroscopic technique when the centres are electrically inactive. LVM spectroscopy is a sensitive tool to study the properties of the corresponding centres and there have been many reviews on the subject (see, for instance, [101]). Vibrational spectroscopy is based on the displacement of atomic masses and the LVMs display isotope shifts when the FAs have several natural isotopes with comparable concentrations, or whose concentrations can be adjusted. These isotope shifts either due to the FAs themselves or to their *nn*s, are of a great help in the chemical identification of the FAs and in the determination of their local environment. The vibrational properties also lend themselves to many theoretical approaches which assist in determining the atomic form of the centre. It must be added that some of the centres showing LVMs in the near or medium IR can also present low-frequency quasi-rotational modes that give absorption in the far IR, and in this latter domain, phonon spectroscopy, whose principles are briefly described at the end of Sect. 3.1, has also been used. Vibrational absorption spectroscopy is a very general method which requires only a vibrational mode of appropriate symmetry for the existence of a dipole moment, and it allows the detection of electrically active as well as electrically inactive or compensated centres. In the absence of a dipole moment, a change of the polarizability of the bond allows the detection of the vibrational mode by Raman scattering. Electrically active FAs or defects display at least two charge states, and different charge states can change the frequencies of the LVMs. This can be seen clear in the case of centres with levels relatively deep in the band gap, where the bound electron or hole is localized on the centre, like for the oxygen-vacancy centre in silicon, but for centres where the bound carrier is more delocalized, the situation may not be so simple.

One drawback of vibrational spectroscopy is its slightly lower sensitivity compared to electronic absorption, thus requiring higher impurity concentrations (in the best cases, the sensitivity limit is however in the 10^{13} – 10^{14} cm⁻³ range), and Raman scattering is still less sensitive.

Small foreign molecules, ions, or free radicals located at an interstitial or more rarely substitutional site, with much less vibrational interaction with the crystal, can also be encountered in semiconductors. The vibration frequencies of such centres are often comparable to the ones in vacuum and they can also display hindered rotation. Ions like OH⁻ [102] or CN⁻ [103] are often found in ionic crystals, where they replace an anion, and their dynamical properties can have similarities with the above centres or with molecules in rare gas matrices. We shall see that they can also be found at interstitial sites in compound semiconductors. Another example is molecular hydrogen in semiconductors, whose vibrational properties are presented in Sect. 8.3.

As already mentioned, the coupling between the electronic and vibrational motions (vibronic coupling) results sometimes in the observation of local modes

replicas of PL lines. The study of these replicas, or vibronic transitions, can supplement the direct absorption measurements as some of the LVMs associated with the vibronic transitions are usually IR inactive and undetectable in pure vibrational absorption.

1.7 Spin Effects

Electron spin effects are observed for electrically active centres with an odd number of electrons. In charge states with an even number of electrons, the spins are generally paired off. There are however a few cases where a two-electron centre gives a resultant spin $S = 1$, with parallel individual spins. A centre in a charge state with nonzero spin is said to be paramagnetic. Such a centre interacts with an external magnetic field \mathbf{B} through the magnetic dipole moment of the electron arising from the electron spin and from its angular momentum. For many centres, the angular momentum of the electron is quenched in the ground state so that one can only consider the spin. In a solid, the Zeeman term can then be expressed as [104]:

$$H_{Zee} = \mu_B \mathbf{gSB},$$

where μ_B is the Bohr magneton and \mathbf{g} a symmetric tensor whose values g_1 , g_2 , and g_3 with respect to the principal axes (the g factors) of the \mathbf{g} tensor are close to 2. The ground state of a centre with spin $S = 1/2$ is split by the magnetic field into a doublet with $M_S = +1/2$ and $-1/2$ separated by $\mu_B \mathbf{gB}$ [for a magnetic field of 1 T and $g \sim 2$, this separation is ~ 30 GHz (~ 0.12 meV)] and a magnetic dipole transition can take place between the two components. We have seen that noncubic centres with different equivalent orientations in a cubic crystal present an orientational degeneracy. When these centres are paramagnetic, the doublet separation depends on the angle between the magnetic field and the main axis of the centres. In classical ESR experiments, the transition between the two levels is induced by the magnetic field of a microwave with a fixed frequency for a critical value of \mathbf{B} . Practically, \mathbf{B} , oriented along a high-symmetry axis of the crystal ($\langle 100 \rangle$, $\langle 111 \rangle$, or $\langle 110 \rangle$) is tuned in order to make the splittings of the centres with different orientations coincide with the microwave frequency and this is repeated for different orientations. The variation of the number of resonances for different orientations of \mathbf{B} allows then the orientational degeneracy of the centre to be determined.

A paramagnetic atom with T_d symmetry should give only one resonance line, but when this atom has a nuclear spin, the electron and nuclear spins can couple by hyperfine interaction, and for a nuclear spin \mathbf{I} , each electronic spin component splits into $2I + 1$ components giving the same number of $\Delta m_I = 0$ resonances. For instance, the ESR spectrum of tetrahedral interstitial Al ($\mathbf{I} = 5/2$) produced by electron irradiation of Al-doped silicon is an isotropic sextuplet due to transitions between the six nuclear sublevels of each electronic-spin component ([104], and references therein). The electron spin of a centre can also interact with the nuclear

spins of neighbouring atoms to give additional structures and this is clearly shown for ^{29}Si atoms ($I = 1/2$) in Fig. 1.4 of the chapter by Watkins [104]. This shows that the analysis of the hyperfine structure of the ESR spectrum can inform on the chemical nature of the atoms involved in the paramagnetic centre. This can also occur for noncubic centres and the hyperfine structure is superimposed to the orientational structure.

For a given value of \mathbf{B} , the energies of the $\Delta m_I = 1$ transitions between the nuclear sublevels of a given electronic spin state are much lower than those between the electronic spin components. Information on the amplitude at different lattice sites in the vicinity of the centre of the wavefunction of the electron whose spin is responsible for the ESR spectrum was obtained by Feher [105] by monitoring the ESR spectrum as a function of the frequencies in the nuclear frequencies range and this technique was called electron nuclear double resonance (ENDOR). Improvements in the sensitivity of ESR can be obtained by using optical or electrical detection methods [106].

All the neutral single donors without d or f electrons have spin $1/2$ while the double donors and acceptors have spin 0 in the ground state, but in some excited states, they have spin 1 and optically forbidden transitions between the singlet and triplet states have been observed. The spins of the neutral acceptors in the ground state depend on the electronic degeneracy of the valence band at its maximum. For silicon, the threefold degeneracy of the valence band results in a quasi-spin $3/2$ of the acceptor ground state. In the high-spin configuration, the spin in the ground state of TMs with configurations d^n goes from $1/2$ to $5/2$ for configurations d^1 to d^5 decreasing from 2 to $1/2$ from configurations d^6 to d^9 .

Useful correlations have been often made between the ESR and optical spectra based on the similarities in the observation conditions, and these correlations have contributed identifying these spectra with specific centres.

1.8 Labelling of the Spectroscopic Signatures

The optical absorption, PL, ESR, and DLTS signatures of a multitude of centres have been reported in semiconductors and insulators, and many solutions to the problem of labelling and identifying these signatures have been used. In the few cases where the identification was established very early, as for the LVMs of interstitial oxygen in silicon, the signatures could be labelled by the atomic configuration of the centre. Such a situation is however met for only a few centres and practical solutions have had to be found.

For instance, a still used nomenclature of the first ZPLs observed in diamond, summarized in Table 3 of [107], was introduced by Clark et al. [108, 109], where prefixes N, GR, R, TR, and H followed by integers correspond to: Naturally occurring (centres occurring in natural diamonds), general radiation (centres induced in all diamonds by irradiation), radiation, type (II) radiation (centres not observed

in type-I diamonds), and heat (centres produced by heat treatment preceded by irradiation), respectively.

At the beginning, unknown ESR spectra in silicon were labelled, for instance, by capital letters, like *A* and *E* by Watkins et al. [110]. In many cases, when an optical signature which could be correlated with the ESR spectrum was observed, the ESR labelling was kept for the optical labelling. This is illustrated by the Si-*A* centre in silicon (there are five different *A* centres in different semiconductor crystals!) named after the ESR spectrum, and characterized by a LVM at 12 μm , which was identified as the *V*O defect [111]. Later, in the ESR world, when an unidentified ESR spectrum was first observed, it was often the rule to label it by the initials of the laboratory, city, or country of the discoverers and by an integer corresponding to the order of discovery. With this method, there was no physical relation between the ESR label in different materials as a similarity in the labels did not mean necessarily a similarity in the nature of the centres: for instance, the C-P1 ESR spectrum in diamond, associated with substitutional nitrogen, was reported first by Smith et al. [112] from the IBM Research Laboratory located then at Poughkeepsie (NY). On the other hand, the Si-P1 ESR spectrum in silicon, first reported by Jung and Newell [113] from Purdue University, was later shown to be due to a non-planar five-vacancy cluster.

Levels found in DLTS measurements were also labelled for discrimination purposes, like the labellings of the EBN and ELN levels ($N = 1, 2, 3, \dots$) of electron traps in GaAs by Martin et al. [114], where B was for Bell Telephone Laboratories and L for Laboratoires d'Électronique et de Physique appliquée (LEP), and from which, incidentally, emerged the EL2 centre. More generally, this led to the naming of spectra or lines by letters, acronyms, or energies of the transition. In many cases, even when the atomic structures of the centres have been properly identified, the old labellings can still be found in some publications. This labelling problem is not trivial and it has been seriously considered [115].

In this book, on the basis of the present knowledge, when possible the centres are labelled on the basis of their atomic structure, but the usual label is generally indicated. When the exact structure is not simple and when there exists an acronym for the centre, it has been used. When admitted labels are associated to transitions of a given centre and when there are no physical attributions to these transitions, we use also the current label.

Several lines or bands have also been denoted by their rounded wavelengths, wavenumbers, or energies, and there has been small changes in the quoted values when wavelength calibration improved, due mainly to the change from dispersive spectrometers needing external calibration to FTSs with built-in calibration. It can thus occur in this book that slightly different rounded values are found for the same band or line. As a rule, the values to take in consideration at a given temperature are those given in the tables, with eventually the proper reference; the unquoted spectral values in the tables are unpublished values of the authors.

Another point to consider is that the same centre can produce more than one spectroscopic feature and these features have to be identified adequately. This is often the case with the different vibrational modes of a given centre. When

these modes are properly identified, they are generally labelled by the irreducible representation(s) of the symmetry point group of the centre to which they belong. Otherwise, they are denoted by their wavenumber.

References

1. M. Balkanski, R.F. Wallis, *Semiconductor Physics and Applications* (Oxford University Press, Oxford, 2000)
2. P.Y. Yu, M. Cardona, *Fundamentals of Semiconductors*, 3rd edn. (Springer, Berlin, 2001)
3. G. Davies, Optical measurements of point defects in semiconductors, in *Identification of Defects in Semiconductors, Semiconductors and Semimetals*, vol. 51B, ed. by M. Stavola (Academic, San Diego, 1999), pp. 1–92
4. K. Nassau, *The Physics and Chemistry of Color: The Fifteen Causes of Color*, 2nd edn. (Wiley-VCH, New York, 2001)
5. T.S. Moss, *Optical Properties of Semi-conductors* (Butterworths, London, 1969)
6. R.C. Newman, *Infrared Studies of Crystal Defects* (Taylor and Francis, London, 1973)
7. B. Pajot, *Optical Absorption of Impurities and Defects in Semiconducting Crystals. I. Hydrogen-Like Centres* (Springer, Berlin, 2010)
8. V.I. Anisimov, M.A. Korotin, E.Z. Kurmaev, Band-structure description of Mott insulators (NiO, MnO, FeO, CoO). *J. Phys. Cond. Matter* **2**, 3973–3987 (1990)
9. N.F. Mott, *Metal-Insulators Transitions* (Taylor and Francis, London, 1974)
10. K. Iakoubovskii, G.J. Adriaenssens, Optical characterization of natural Argyle diamonds. *Diam. Relat. Mater.* **11**, 125–131 (2002)
11. A.T. Collins, The detection of colour-enhanced and synthetic gem diamonds by optical spectroscopy. *Diam. Relat. Mater.* **12**, 1976–1983 (2003)
12. B.O. Kolbesen, A. Mühlbauer, Carbon in silicon: properties and impact on devices. *Solid State Electron.* **25**, 759–775 (1982)
13. J. Czochralski, Ein neues verfahren zur messung der kristallisationsgeschwindigkeit. *Z. Phys. Chem.* **92**, 219–221 (1918)
14. W. Lin, The incorporation of oxygen into silicon crystals, in *Oxygen in Silicon, Semiconductors and Semimetals*, vol. 42, ed. by F. Shimura (Academic, San Diego, 1994), pp. 9–52
15. W. Ulrici, F.M. Kiessling, P. Rudolph, The nitrogen-hydrogen-vacancy complex in GaAs. *Phys. Stat. Sol. B* **241**, 1281–1285 (2004)
16. V. Clerjaud, D. Côte, C. Naud, M. Gauneau, R. Chaplain, Unintentional hydrogen concentration in liquid encapsulation Czochralski grown III-V compounds. *Appl. Phys. Lett.* **59**, 2980–2982 (1991)
17. W. Keller, A. Mühlbauer, *Floating-Zone Silicon. Preparation and Properties of Solid State Materials*, vol. 5 (Marcel Dekker, New York, 1981)
18. B. Schaub, J. Gallet, A. Brunet-Jailly, B. Pellicciari, Preparation of cadmium telluride by a programmed solution growth technique. *Rev. Phys. Appl.* **12**, 147–150 (1977)
19. K. Iakoubovskii, G.J. Adriaenssens, M. Nesladek, Photochromism of vacancy-related centres in diamond. *J. Phys. Condens. Matter* **12**, 189–199 (2000)
20. A.T. Collins, Spectroscopy of defects and transition metals in diamond. *Diam. Relat. Mater.* **9**, 417–423 (2000)
21. E.F. Schubert, *Doping in III-V Compound Semiconductors* (Cambridge University Press, Cambridge, 2005)
22. J.W. Cleland, K. Lark-Horovitz, J.C. Pigg, Transmutation produced germanium semiconductors. *Phys. Rev.* **78**, 814–815 (1950)
23. M. Kato, T. Yoshida, Y. Ikeda, Y. Kitagawara, Transmission electron microscope observation of “IR scattering defects” in as-grown Czochralski Si crystals. *Jpn. J. Appl. Phys.* **35**, 5597–5601 (1996)

24. F. Spaepen, A. Eliat, New methods for determining the void content of silicon single crystals. *IEEE Trans. Instrum. Meas.* **48**, 230–232 (1999)
25. H. Yamada-Kaneta, T. Goto, Y. Nemoto, K. Sato, M. Hikin, Y. Saito, S. Nakamura, Vacancies in CZ silicon crystal observed by low-temperature ultrasonic measurements. *Physica B* **401–402**, 138–143 (2007)
26. G.M. Martin, Optical assessment of the main electron trap in bulk semi-insulating gallium arsenide. *Appl. Phys. Lett.* **39**, 747–748 (1981)
27. J.C. Bourgoin, H.J. von Bardeleben, D. Stiévenard, Native defects in gallium arsenide. *J. Appl. Phys.* **64**, R65–R91 (1988)
28. Z.Q. Chen, S. Yamamoto, M. Maekawa, A. Kawasuso, Postgrowth annealing of defects in ZnO studied by positron annihilation, x-ray diffraction, Rutherford backscattering, cathodoluminescence and Hall measurements. *J. Appl. Phys.* **94**, 4807–4812 (2003)
29. P. Wagner, J. Hage, Thermal double donors in silicon. *Appl. Phys. A* **49**, 123–128 (1989)
30. P. Clauws, Oxygen-related defects in germanium. *Mater. Sci. Eng. B* **36**, 213–220 (1996)
31. C.A.J. Ammerlaan, Shallow thermal donors in c-Si, in *Properties of Crystalline Silicon, EMIS Data Reviews Series No. 20*, ed. by R. Hull (INSPEC, London, 1999), pp. 659–662
32. J.W. Corbett, G.D. Watkins, Silicon divacancy and its direct production by electron irradiation. *Phys. Rev. Lett.* **7**, 314–316 (1961)
33. G.D. Watkins, The lattice vacancy in silicon, in *Deep Centers in Semiconductors*, 2nd edn., ed. by S.T. Pantelides (Gordon and Breach, New York, 1992), pp. 177–213
34. G.G. DeLeo, W.B. Fowler, G.D. Watkins, Theory of off-center impurities in silicon: substitutional nitrogen and oxygen. *Phys. Rev. B* **29**, 3193–3207 (1984)
35. L.I. Murin, B.G. Svensson, J.L. Lindström, V.P. Markevich, C.A. Londos, Trivacancy-oxygen complex in silicon: local vibrational mode characterization. *Physica B* **404**, 4568–4571 (2009)
36. D.J. Chadi, K.J. Chang, Magic numbers for vacancy aggregation in crystalline Si. *Phys. Rev. B* **38**, 1523–1525 (1988)
37. S.K. Estreicher, J.L. Hastings, P.A. Fedders, The ring-hexavacancy in silicon: a stable and inactive defect. *Appl. Phys. Lett.* **70**, 432–434 (1997)
38. B. Hourahine, R. Jones, A.N. Safonov, S. Öberg, P.R. Briddon, S.K. Estreicher, Identification of the hexavacancy in silicon with the B_{80}^4 optical center. *Phys. Rev. B* **61**, 12584–12597 (2000)
39. J. Chevallier, B. Pajot, Interaction of hydrogen with impurities and defects in semiconductors. *Solid State Phenom.* **85–86**, 203–284 (2002)
40. S.R. Wilson, W.M. Paulson, W.F. Krolikowski, D. Fathy, J.D. Gressett, A.H. Hamdi, F.D. McDaniel, Characterization of n-type layers formed in Si by ion implantation of hydrogen, in *Proceedings of Symposium on Ion Implantation and Ion Beam Processing of Materials*, ed. by G.K. Hubler, O.W. Holland, C.R. Clayton, C.W. White (North Holland, New York, 1984), pp. 287–292
41. R. Jones, S. Öberg, F. Berg Rasmussen, B. Bech Nielsen, Identification of the dominant nitrogen defect in silicon. *Phys. Rev. Lett.* **72**, 1882–1885 (1994)
42. P. Humble, D.F. Lynch, A. Olsen, Platelets defects in natural diamond. II. Determination of structure. *Phil. Mag.* **52**, 623–641 (1985)
43. J.P. Goss, B.J. Coomer, R. Jones, T.D. Shaw, P.R. Briddon, M. Rayson, S. Öberg, Self-interstitial aggregation in diamond. *Phys. Rev.* **63**, 195208/1–14 (2001)
44. D.G. Thomas, J.J. Hopfield, Isoelectronic traps due to nitrogen in gallium phosphide. *Phys. Rev.* **150**, 680–689 (1966)
45. R.C. Newman, R.S. Smith, Local mode absorption from boron complexes in silicon, in *Localized Excitations in Solids*, ed. by R.F. Wallis (Plenum, New York, 1968), pp. 177–184
46. S.R. Morrisson, R.C. Newman, F. Thompson, The behaviour of boron impurities in n-type gallium arsenide and gallium phosphide. *J. Phys. C* **7**, 633–644 (1974)
47. M. Hiller, E.V. Lavrov, J. Weber, Raman scattering study of H_2 in Si. *Phys. Rev. B* **74**, 235214/1–9 (2006)
48. L. Vegard, Die Konstitution der Mischkristalle und die Raumfüllung der Atome. *Z. Phys.* **5**, 17–26 (1921)

49. A.R. Denton, N.W. Ashcroft, Vegard's law. *Phys. Rev. A* **43**, 3161 (1991)
50. K.G. McQuhae, A.S. Brown, The lattice contraction coefficient of boron and phosphorus in silicon. *Solid State Electron.* **15**, 259–264 (1972)
51. Y. Takano, M. Maki, Diffusion of oxygen in silicon, in *Semiconductor Silicon 1973*, ed. by H.R. Huff, R.R. Burgess (The Electrochemical Society, Pennington, 1973), pp. 469–481
52. D. Windisch, P. Becker, Silicon lattice parameters as an absolute scale of length for high-precision measurements of fundamental constants. *Phys. Stat. Sol. A* **118**, 379–388 (1990)
53. J.E. Rowe, F. Sette, S.J. Pearton, J.M. Poate, Local structure of DX-like centers from extended x-ray absorption fine structure. *Diffusion and Defect Data Part B. Solid State Phenom.* **10**, 283–295 (1990)
54. K.L. Kavanagh, G.S. Gargill III, Lattice strain from substitutional Ga and from holes in heavily doped Si:Ga. *Phys. Rev. B* **45**, 3323–3331 (1992)
55. S. Wei, H. Oyonagi, H. Kawanami, T. Sakamoto, K. Tamura, N.L. Saini, K. Uosaki, Local structure of isovalent and heterovalent dilute impurities in Si crystal probed by fluorescence X-ray absorption fine structure. *J. Appl. Phys.* **82**, 4810–4815 (1997)
56. B. Pajot, A.M. Stoneham, A spectroscopic investigation of the lattice distortion at substitutional sites for group V and VI donors in silicon. *J. Phys. C Solid State Phys.* **20**, 5241–5252 (1987)
57. E. Gaudry, A. Kiratisin, P. Sainctavit, C. Brouder, F. Mauri, A. Ramos, A. Rogale, J. Goulon, Structural and electronic relaxation around substitutional Cr^{3+} and Fe^{3+} in corundum. *Phys. Rev. B* **67**, 094108 (2003)
58. M. Hakala, M.J. Puska, R.M. Nieminen, First-principle calculations of interstitial boron in silicon. *Phys. Rev. B* **61**, 8155–8161 (2000)
59. D. Sasireka, E. Palanyandi, K. Yakutti, Study of local lattice relaxation of substitutional impurities in silicon and germanium. *Int. J. Quant. Chem.* **99**, 142–152 (2004)
60. T. Sugiyama, K. Tanimura, N. Itoh, Direct measurement of transient macroscopic volume change induced by generation of electron-hole pairs in GaP and GaAs. *Appl. Phys. Lett.* **58**, 146–148 (1990)
61. B. Pajot, Solubility of O in silicon, in *Properties of Crystalline Silicon, EMIS Data Reviews Series No. 20*, ed. by R. Hull (INSPEC, London, 1999), pp. 488–491
62. J.C. Mikkelsen Jr., The diffusivity and solubility of oxygen in silicon. *Mater. Res. Soc. Symp. Proc.* **59**, 19–30 (1986)
63. W. Kaiser, C.D. Thurmond, Solubility of oxygen in germanium. *J. Appl. Phys.* **32**, 115–118 (1961)
64. R. Duffy, T. Dao, Y. Tamminga, K. van der Tak, F. Roozeboom, E. Augendre, Group III and V impurity solubilities in silicon due to laser, flash, and solid-phase-epitaxial-regrowth. *Appl. Phys. Lett.* **89**, 071915 (2006)
65. W. Schröter, M. Seibt, Solubility and diffusion of transition metal impurities in c-Si, in *Properties of Crystalline Silicon, EMIS Data Reviews Series No. 20*, ed. by R. Hull (INSPEC, London, 1999), pp. 543–560
66. R.C. Young, J.W. Westhead, J.C. Corelli, Interaction of Li and O with radiation-produced defects in Si. *J. Appl. Phys.* **40**, 271–278 (1969)
67. T. Nozaki, Y. Yatsurugi, N. Akiyama, Y. Endo, Y. Makide, Behaviour of light impurity elements in the production of semiconductor silicon. *J. Radioanal. Chem.* **19**, 109 (1974)
68. A.R. Bean, R.C. Newman, The solubility of carbon in pulled silicon crystals. *J. Phys. Chem. Solids* **32**, 1211–1219 (1971)
69. W.R. Runyan, *Silicon Semiconductor Technology, Texas Instruments Electronic Series* (McGraw Hill, New York, 1965)
70. W. Rosnowski, Aluminium diffusion into silicon in an open tube high vacuum system. *J. Electrochem. Soc.* **125**, 957–962 (1978)
71. J.S. Makris, B.J. Masters, Phosphorus isoconcentration diffusion studies in silicon. *J. Electrochem. Soc.* **120**, 1252–1255 (1973)
72. F. Rollert, N.A. Stolwijk, H. Mehrer, Diffusion of sulfur-35 into silicon using an elemental vapor source. *Appl. Phys. Lett.* **63**, 506–508 (1993)

73. S.J. Pearton, Alkali impurities (Na, K, Li) in c-Si, in *Properties of Crystalline Silicon*, EMIS Data Reviews Series No. 20, ed. by R. Hull (INSPEC, London, 1999), pp. 593–595
74. A. Mesli, T. Heiser, Interstitial defect reactions in silicon: the case of copper. *Defect and Diffusion Forum* 131–132 (Trans Tech, Liechtenstein, 1996), p. 89
75. T. Isobe, H. Nakashima, K. Hashimoto, Diffusion coefficient of interstitial iron in silicon. *Jpn. J. Appl. Phys.* **28**, 1282–1283 (1989)
76. S. Hocine, D. Mathiot, Titanium diffusion in silicon. *Appl. Phys. Lett.* **53**, 1269–1271 (1988)
77. R.C. Newman, J. Wakefield, The diffusivity of carbon in silicon. *J. Phys. Chem. Solids* **19**, 230–234 (1961)
78. R. Hull (ed.), *Properties of Crystalline Silicon*, EMIS Data Reviews Series No. 20 (INSPEC, London, 1999)
79. H. Mehrer, *Diffusion in Solids – Fundamentals, Methods, Materials, Diffusion-Controlled Processes* (Springer, Berlin, 2007)
80. C. Herring, N.M. Johnson, Hydrogen migration and solubility in silicon, in *Hydrogen in Semiconductors*, ed. by J.I. Pankove, N.M. Johnson, *Semiconductors and Semimetals*, ed. by R.K. Willardson, A.C. Beer (Academic, Boston, 1991), pp. 225–350
81. C.T. Sah, J.Y.C. Sun, J.J.T. Tzou, Deactivation of the boron acceptor in silicon by hydrogen. *Appl. Phys. Lett.* **43**, 204–206 (1983)
82. J.I. Pankove, D.E. Carlson, J.E. Berkeyheiser, R.O. Wance, Neutralization of shallow acceptor levels in silicon by atomic hydrogen. *Phys. Rev. Lett.* **51**, 2224–2225 (1983)
83. J.H. Svernnson, B.G. Svernnson, B. Monemar, Infrared absorption studies of the divacancy in silicon: new properties of the singly negative charge state. *Phys. Rev. B* **38**, 4192–4197 (1988)
84. P.W. Anderson, Model for the electronic structure of amorphous semiconductors. *Phys. Rev. Lett.* **34**, 953–955 (1975)
85. H.Ch. Alt, Experimental evidence for a negative- U center in gallium arsenide related to oxygen. *Phys. Rev. Lett.* **65**, 3421–3424 (1990)
86. M. Pesola, J. von Boehm, V. Sammalkorpi, T. Mattila, R.M. Nieminen, Microscopic structure of oxygen defects in gallium arsenide. *Phys. Rev. B* **60**, R16267–R16270 (1999)
87. J.R. Troxell, G.D. Watkins, Interstitial boron in silicon: a negative- U system. *Phys. Rev. B* **22**, 921–931 (1980)
88. R.D. Harris, J.L. Newton, G.D. Watkins, Negative- U defect: interstitial boron in silicon. *Phys. Rev. B* **36**, 1094–1104 (1987)
89. A.A. Istratov, H. Hielsmair, E.R. Weber, Iron and its complexes in silicon. *Appl. Phys. A* **69**, 13–44 (1999)
90. T. Dietl, A ten-year perspective on dilute magnetic semiconductors and oxides. *Nat. Mater.* **9**, 966–974 (2010)
91. K. Akimoto, H. Okuyama, M. Ikeda, Y. Mori, Isoelectronic oxygen in II–VI compounds. *Appl. Phys. Lett.* **60**, 91–93 (1992)
92. P.J. Dean, R.A. Faulkner, Zeeman effect and crystal-field splitting of excitons bound to isoelectronic bismuth in gallium phosphide. *Phys. Rev.* **185**, 1064–1067 (1969)
93. A.M. White, P.J. Dean, K.M. Fairhurst, W. Bardsley, B. Day, The Zeeman effect in the spectrum of exciton bound to isoelectronic bismuth in indium phosphide. *J. Phys. C Solid State Phys.* **7**, L35–L39 (1974)
94. M.L.W. Thewalt, D. Labrie, T. Timusk, The far infrared spectra of bound excitons in silicon. *Solid State Commun.* **53**, 1049–1054 (1985)
95. G.D. Watkins, Vacancies and interstitials and their interactions with other defects in silicon, in *Proceeding of Third International Symposium on Defects in Silicon*, *Electrochem. Soc. Symp. Proc.*, vol. 99–1, ed. by T. Abe, W.M. Bullis, S. Kobayashi, W. Lin, P. Wagner (Electrochemical Society, Pennington, 1999), pp. 38–52
96. T.V. Mashovets, V.V. Emtsev, Point defects in germanium, in *Inst. Phys. Conf. Ser. No. 23* (The Institute of Physics, Bristol, 1975), pp. 103–125
97. P.J. Dean, J.R. Haynes, W.F. Flood, New radiative recombination processes involving neutral donors and acceptors in silicon and germanium. *Phys. Rev.* **161**, 711–729 (1967)

98. G. Davies, The optical properties of luminescence centers in silicon. *Phys. Rep.* **176**, 83–188 (1989)
99. B. Monemar, U. Lindefelt, W.M. Chen, Electronic structure of bound excitons in semiconductors. *Physica B & C* **146**, 256–285 (1987)
100. J.F. Angress, A.R. Goodwin, S.D. Smith, A study of the vibrations of boron and phosphorus in silicon by infrared absorption. *Proc. Roy. Soc. Lond. A* **287**, 64–68 (1965)
101. M.D. McCluskey, Local vibrational modes of impurities in semiconductors. *J. Appl. Phys.* **87**, 3593–3617 (2000)
102. C.K. Chau, M.V. Klein, B. Wedding, Photon and phonon interactions with OH^- and OD^- in KCl. *Phys. Rev. Lett.* **17**, 521–525 (1966)
103. R.C. Spitzer, W.P. Ambrose, A.J. Sievers, Observation of persistent hole burning in the vibrational spectrum of CN in KBr. *Phys. Rev. B* **34**, 7307–7317 (1986)
104. G.D. Watkins, EPR and ENDOR studies of defects in semiconductors, in *Identification of Defects in Semiconductors, Semiconductors and Semimetals*, vol. 51A, ed. by M. Stavola (Academic, San Diego, 1998), pp. 1–43
105. G. Feher, Electron spin resonance experiments on donors in silicon. I. Electronic structure of donors by the electron nuclear double resonance technique. *Phys. Rev.* **114**, 1219–1244 (1959)
106. J.M. Spaeth, Magneto-optical and electrical detection of paramagnetic resonance in semiconductors, in *Identification of Defects in Semiconductors, Semiconductors and Semimetals*, vol. 51A, ed. by M. Stavola (Academic, San Diego, 1998), pp. 45–92
107. J. Walker, Optical absorption and luminescence in diamond. *Rep. Prog. Phys.* **42**, 1605–1659 (1979)
108. C.D. Clark, R.W. Ditchburn, H.B. Dyer, The absorption spectra of natural and irradiated diamond. *Proc. R. Soc. Lond. A* **234**, 363–381 (1956)
109. C.D. Clark, R.W. Ditchburn, H.B. Dyer, The absorption spectra of irradiated diamonds after heat treatment. *Proc. Roy. Soc. Lond. A* **237**, 75–89 (1956)
110. G.D. Watkins, J.W. Corbett, R.M. Walker, Spin resonance in electron irradiated silicon. *J. Appl. Phys.* **30**, 1198–1203 (1959)
111. J.W. Corbett, G.D. Watkins, R.M. Chrenko, R.S. McDonald, Defects in irradiated silicon. I. Infrared absorption of the Si-A center. *Phys. Rev.* **121**, 1015–1022 (1961)
112. W.V. Smith, P.P. Sorokin, I.L. Gelle, G.J. Lasher, Electron-spin resonance of nitrogen donors in diamond. *Phys. Rev.* **115**, 1546–1552 (1959)
113. W. Jung, G.S. Newell, Spin-1 centers in neutron-irradiated silicon. *Phys. Rev.* **132**, 648–662 (1963)
114. G.M. Martin, A. Mitonneau, A. Mircea, Electron traps in bulk and epitaxial GaAs crystals. *Electron. Lett.* **13**, 191–192 (1977)
115. F. Bridges, G. Davies, J. Robertson, A.M. Stoneham, The spectroscopy of crystal defects: a compendium of defect nomenclature. *J. Phys. Cond. Matter* **2**, 2875–2928 (1990)

Optical Absorption of Impurities and Defects in
Semiconducting Crystals
Electronic Absorption of Deep Centres and Vibrational
Spectra

Pajot, B.; Clerjaud, B.

2013, XXVIII, 512 p., Hardcover

ISBN: 978-3-642-18017-0